

Carbon Balance and Forest Dynamics in an Old-growth Amazonian Forest

A Thesis
Presented to the Department of Biology
Harvard University
By Ann Rice
In Partial Fulfillment of the Requirements
For the Degree of
Bachelor of Arts with Honors
January 2002

Thesis Director: Professor Steven Wofsy
Thesis Sponsor: Professor David Foster

ACKNOWLEDGEMENTS:

I am delighted to acknowledge my two thesis advisors, Professor Steven Wofsy and Professor David Foster, for their invaluable suggestions, comments and criticisms during the thesis writing process. I am grateful to Professor Wofsy for giving me an opportunity to work in a new field, allowing me so much autonomy in my project and encouraging me to think critically. I thank Professor Foster for igniting my interest in forestry, for helping me find a project and for his insightful conversations and guidance.

My thesis would not have been possible without the support of the Wofsy lab. I am indebted to Elizabeth Hammond Pyle; she went above and beyond the call of duty teaching me how to program in S-plus, helping me set up my project, helping me organize my data, editing many drafts of each section of my thesis and challenging me to write powerfully. Scott Saleska and Lucy Hutrya helped me design the coarse woody debris experiment, trained me for my fieldwork and shared their programming wisdom.

I am indebted to all of the people who made my fieldwork in Brazil possible. Bethany Reid, the LBA coordinator, provided personal support and was a logistical wizard with vehicles, computers and personnel. I thank Erly Pedroso and Nilson de Souza Carvalho for sharing their incredible knowledge of the rainforest and for their hard work in the field. I am grateful to Kleber Portilho and Dulcyana Ferreira for their assistance with the coarse woody debris and live biomass surveys.

To my parents, thank you for giving me encouragement, love and chances. To my grandparents, stepparents and sisters, thank you for believing in me, supporting me and pushing me to go further. To my incredible friends, I am grateful for your love, distraction and appreciation of purple hair.

TABLE OF CONTENTS

I. Introduction	4
II. Site Description	8
III. Methodology	14
IV. Results	24
V. Discussion and Conclusions	43
VI. References	53

INTRODUCTION:

Forests contain 80% of live aboveground biomass in the world with over 59% of total live biomass residing in tropical forests (Dixon et al., 1994). Tropical forests not only store large amounts of carbon, but over a period of 25 years they cycle a volume of carbon dioxide equal to the total amount in the atmosphere (Mahli & Grace, 2000) and account for as much as 35% of global net primary production (Mellilo et al., 1993). Due to their tremendous capacity for storage and cycling of carbon, small changes in net carbon balance or land use change in tropical forests can result in significant storage or release of carbon dioxide to the atmosphere.

The concentration of carbon dioxide has increased in the atmosphere since the Industrial Revolution (Keeling et al., 1996). This increase is largely the result of the burning of fossil fuels with a significant contribution (23%) from deforestation (Dixon et al., 1994). In the 1990s, the atmosphere received an annual average of 7.9 ± 1.2 Gt C (Prentice et al., 2001) from fossil fuels; however, only 3.2 ± 0.1 Gt C remained in the atmosphere (Prentice et al., 2001). This leaves more than half of the annual carbon dioxide emissions removed by “sinks” widely thought to be in the world’s forests and oceans. There is a great deal of debate over the magnitude and location of the terrestrial sinks (Malhi et al., 1999). Global-atmospheric measurements indicate that temperate and boreal forests in the Northern Hemisphere absorb large amounts of carbon (Fan et al., 1998). However, there is a considerable uncertainty about the role of tropical ecosystems in the global carbon cycle (Melillo et al., 1996; Brown et al., 1993) because the relationships between deforestation, undisturbed forests and the atmospheric exchange are unclear (Tian et al., 2000).

The role of old-growth forests in the tropics remain particularly unclear (Houghton, 1991, Melillo et al., 1993). Are old-growth tropical forests storing carbon and, if so, what are

the pools and fluxes of carbon dioxide within the forest? In the past, primary tropical forests were virtually ignored in terrestrial carbon sink estimates because these forests are predominantly old-growth forests that were assumed to be in a state of dynamic equilibrium (Salati & Vose, 1984). However in recent years, it has been suggested that old-growth neotropical forests are absorbing carbon as a result of carbon dioxide fertilization or nitrogen deposition and that the carbon sink is large enough to offset the carbon released from neotropical deforestation (Phillips et al., 1998; Grace et al., 1995; Chambers et al., 2001b; Tian et al., 2000; Malhi et al., 1998). The carbon sink (per unit area) in old-growth tropical forests is estimated to be somewhere between $0.4 \text{ Mg C ha}^{-1} \text{ yr}^{-1}$ (Tian et al., 2000; Chambers et al., 2001b) and $5.9 \text{ Mg C ha}^{-1} \text{ yr}^{-1}$ (Malhi et al., 1998) or between 0.2 Gt C yr^{-1} and $2.95 \text{ Gt C yr}^{-1}$ if the sink is assumed to extend to all of Amazonia.

There have been three major approaches to understanding the carbon balance of old-growth tropical forests: eddy covariance measurements, ecosystem modeling and biomass inventories. Each of these approaches has strengths and weaknesses.

Eddy covariance studies by Grace et al. (1995) and Malhi et al. (1998) showed significant uptake of carbon. Eddy covariance studies measure whole system carbon dioxide exchange between ecosystems and the atmosphere and are a powerful way of detecting very small changes in whole ecosystem carbon dioxide exchange over short or long time scales. However, both of the above eddy covariance studies were conducted over a short time scale of measurement (55 days, Grace et al. (1995); <1 yr, Malhi et al. (1998)) and have spatial constraints, sampling ~ 100 ha forest. It is problematic to extrapolate up to a regional carbon budget from single field sites, thereby ignoring the spatial and temporal heterogeneity of tropical forests. In addition, eddy covariance studies are limited to aggregated system

measurements and do not address the ecological components of carbon cycling, namely, the balance of different carbon pools and fluxes in the forest.

Ecosystem modeling studies (Tian et al., 2000; Chambers et al., 2001b) parameterize ecosystem characteristics such as species number, wood density, maximum tree size and tree standing stocks, and ecosystem processes such as growth, mortality and decomposition. Theoretically, the approach can avoid the spatial constraints of the eddy covariance studies and can predict basin-wide ecosystem response if the model is parameterized with data from many different locations. However, if the model is parameterized by measurements from a limited spatial area (e.g. Chambers et al., 2001b), then regional extrapolation may cause significant errors. In addition, ecosystem modeling is limited by uncertainties when estimating model parameters and by an incomplete knowledge of ecosystem processes. Often, the key results for modeling studies (e.g. annual carbon change) can not be tested against empirical data.

Biomass inventories such as that by Phillips et al. (1998) attempt to quantify carbon accumulation or release by monitoring tree growth and mortality in long-term forest plots. Biomass inventories can address the specific ecological changes of different forest components over time, but also suffer spatial limitations when scaling up to regional budgets. The Phillips et al. (1998) study was flawed as a biomass inventory because the sites used for measurement were not intended for biomass studies, many plots were small and the plots were not randomly placed because “good looking” forest was often selected (Phillips & Gentry, 1994). There appear to be significant errors in calculation and overestimates of carbon storage because many of the plots selected for measurement were in previously disturbed forests (P. Ashton, personal communication). In addition, most inventories (e.g. Phillips et al., 1998) lack an analysis of other significant biomass pools in the forests. Specifically they neglect dead biomass.

All of these studies suffer from experimental limitations and their estimates of carbon storage in neotropical old-growth forests are far from certain. Further work is imperative to document the role of old-growth neotropical forests in the carbon cycle and to understand the live and dead pools and fluxes of carbon dioxide within an undisturbed neotropical forest.

All three previous approaches ignore forest dynamics, an important component of local, regional and global carbon budgets. Changes in forest demography or successional state can affect the carbon balance in live and dead biomass pools. Demographics and carbon balances can change for extended periods of time with disturbance events such as drought, fire or wind throw. Furthermore, live and dead pools may respond differently to climatic variation and disturbance events. For example, drought may cause a decrease in live biomass and increase in dead biomass because of high mortality and decreased decomposition of dead wood. For an accurate understanding of carbon flux, both pools must be quantified and the dynamics of each analyzed as potential ecological factors driving the carbon budget. Each of these analyses can help reveal the potential disturbance events and climatic factors that affected the site prior to measurement.

The goal of this thesis is to address the issue of carbon storage and release in an old-growth neotropical forest in Pará, Brazil, through detailed biomass studies, carbon budgets and estimation of net carbon flux. This thesis attempts to quantify the pool size and fluxes for live and dead biomass and to contextualize the carbon budget through an analysis of forest dynamics. The project is part of a long-term study at this site that includes eddy correlation flux measurements, remote sensing, atmospheric measurements using aircraft and comparison with a nearby selectively logged site.

SITE DESCRIPTION:

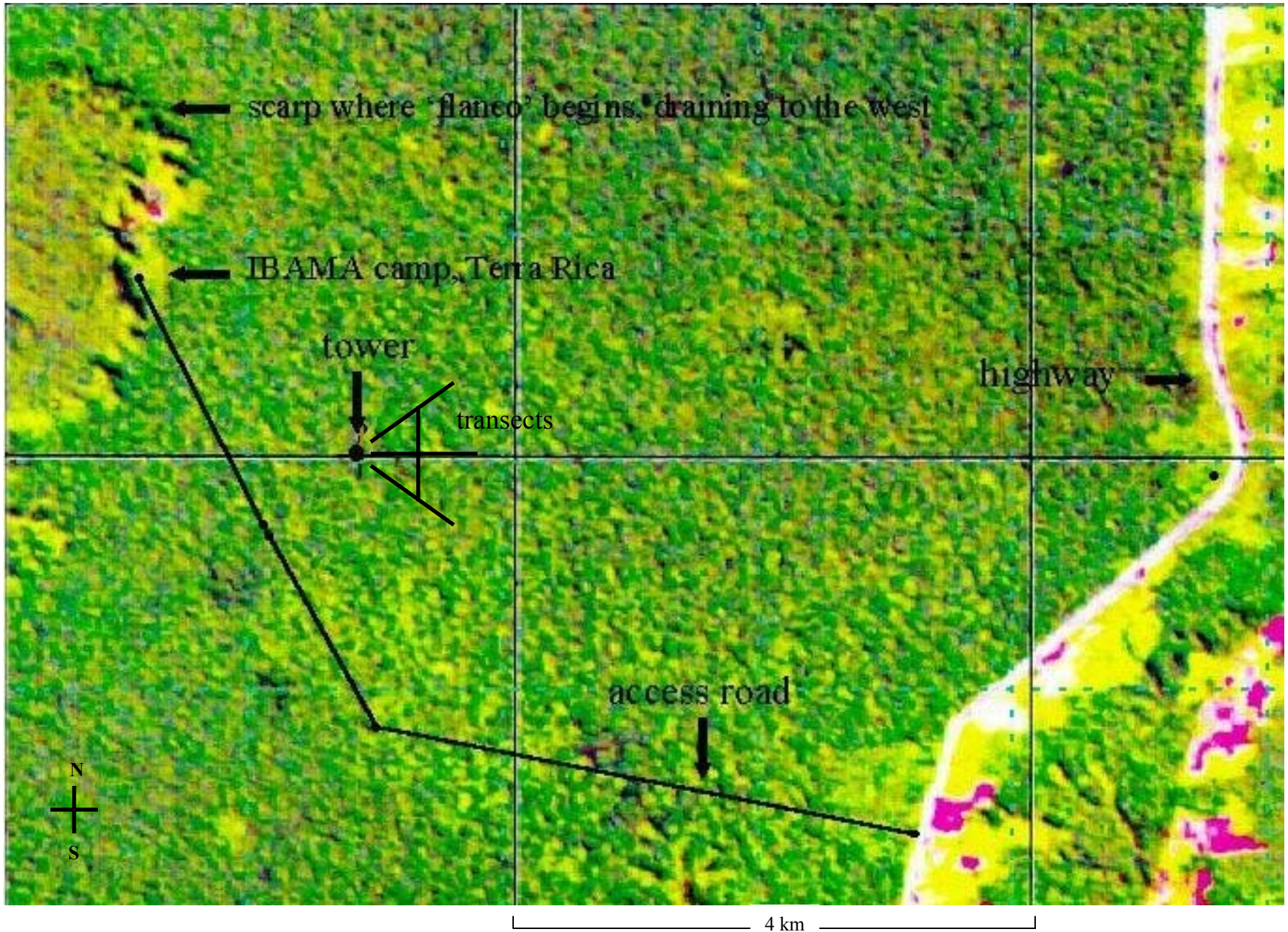
Physical Characteristics

The field site is located in the Tapajós National Forest (54°58'W, 2°51'S) established in 1974 in the state of Pará, Brazil. The site is 2.4 km east of the 80m high escarpment to Tapajós river bed, 7.2 km west of the km 67 Tapajós entrance along the BR-163 Santarém-Cuiaba Highway (est. c1970) and 50 km south of the city of Santarém (Figure 1).

The forest is a closed-canopy upland forest with an average temperature of 25 C, an average humidity of 85% and an average rainfall of 1920 mm a year (Parotta et al., 1995). The wet season in the Tapajós forest occurs between February and June. The dry season is between August and October and the interim season lasts from November to January. Geologically, the region is a part of the lower Amazon/middle basin on zones of ancient uplifted crystalline rock (Parotta et al., 1995). The soils are extremely nutrient poor clay oxisoils, with little organic matter and low cation exchange (Parotta et al., 1995).

The forest is classified as old growth because it does not show recent signs of significant human disturbance, and because of the presence of trees > 70 cm DBH, variable canopy height, epiphytes and large downed wood (Clark, 1996a). With over 260 species, the forest is comparable to the regional average of 200-300 species ha⁻¹ (Malhi et al., 1999). The forest also contains the emergent species that are considered typical for the region (Parotta et al., 1995): *Betholletia excelsa* Humb. & Bonpl., *Couratari* spp., *Hymenaea courbaril* L., *Manilkara huberi*, *Parkia* spp., and *Tabebuia serratifolia* (Vahl) Nichols. The site was selected for study because of the lack of human disturbance, the old-growth classification, the regionally representative forest structure, its accessibility from existing roads and its flat topography (desired for accurate eddy-flux measurements).

Figure 1: 1997 Landsat image of the Tapajós National Forest with the tower, transects and other notable landmarks indicated. The tower is located at (54°58'W, 2°51'S).



Land use and Disturbance History

The natural disturbance regime in the Tapajós encompasses both wind disturbance and fire. Tree mortality from wind-throw is common and constant in the Tapajós; on the site ~20 trees out of 2600 annually die from wind-throw. Natural wildfire in undisturbed closed canopy tropical forests is rare due to the high rainfall and a moist microclimate (Uhl et al., 1988). Fires are typically low intensity with a return interval longer than 1000 years (Cochrane, 1999). In general, modern human activities including road building, slash-and-burn agriculture and forest conversion have caused an increase in frequency and severity of tropical wildfires (Uhl & Buschbacher, 1985). Charcoal fragments discovered in soil pits < 10 km away provide evidence of local fire disturbance (M. Cochrane, personal communication). However, no recent charcoal fragments were found on the km 67 site, indicating a lack of fire disturbance in the immediate area.

There is also a history of human disturbance in the Tapajós both pre- and post-settlement of Santarém. Pottery shards discovered with the charcoal fragments on a nearby site < 10 km away provide evidence of pre-settlement occupation of the Tapajós by indigenous people (M. Cochrane, personal communication). Thus, anthropogenic fire and shifting cultivation associated with native settlements may have altered the Tapajós forest prior to European settlement. This type of disturbance is difficult to detect because of the long time period elapsed since arrival of Europeans. Post-settlement disturbance includes logging as well as resin and fruit extraction. High value trees such as *Manilkara huberi* (Ducke) Chev., *Cedrela odorata* L. and *Aniba roseadora* Ducke were selectively logged during early settlement of Santarém (Parotta et al., 1995). Nevertheless, the km 67 site has many large *Manilkara huberi* and has only one stump of *Manilkara huberi* dating from the 1960's, indicating no recent selective

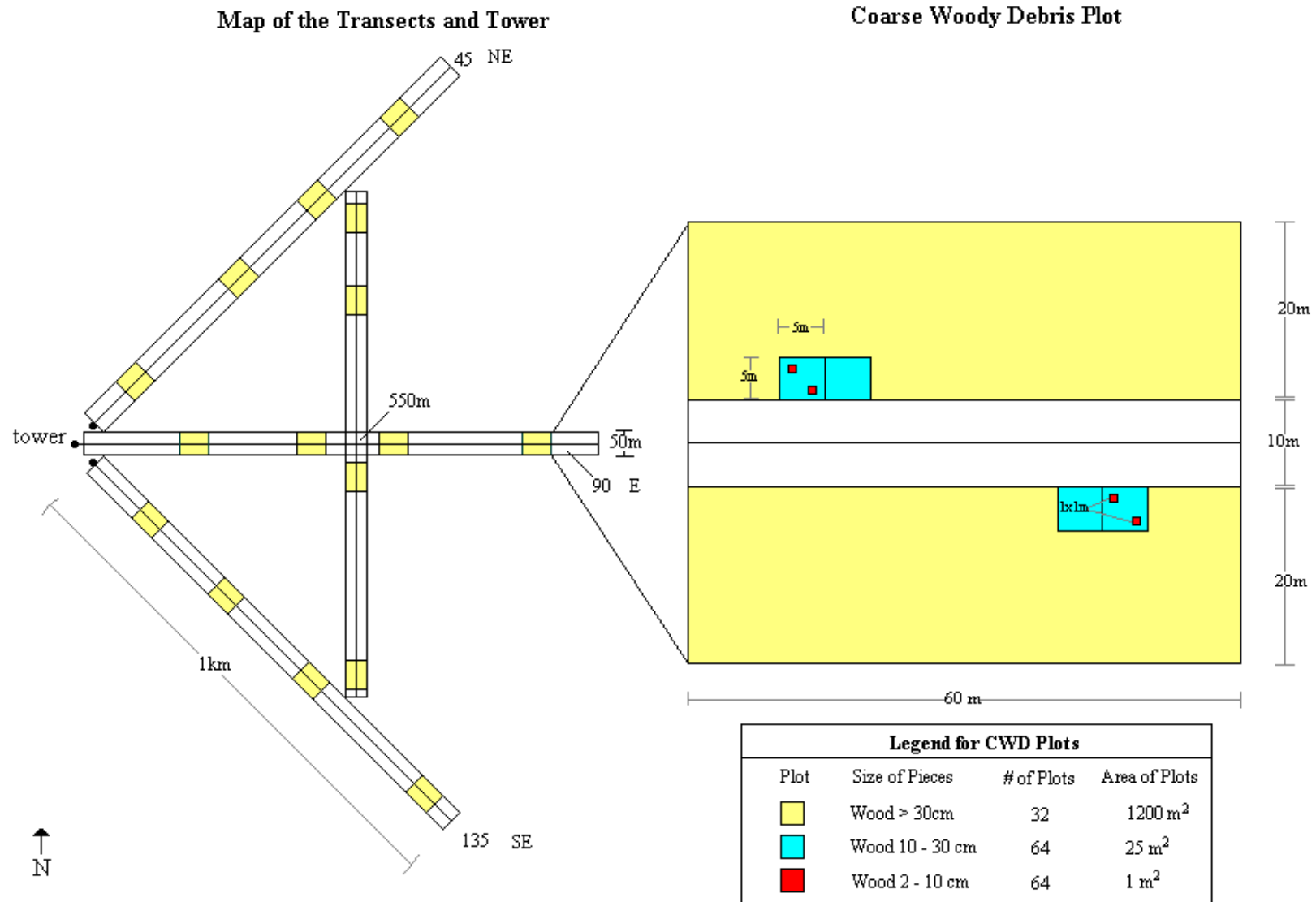
logging. A large number of the Tapajós species yield resins, edible fruits or medicines used for commercial or local consumption (Parotta et al., 1995). Some trees have old scars from resin tapping and there may be a current low level extraction of fruits by local populations, but these actions appear to cause minimal disturbance to a forest and probably do not impact the total carbon budget.

Research Installations

The research installations at the site include an eddy-flux tower, an instrumentation shack and four permanent transects, each 1 km in length, covering 20 ha of forest (Figure 2). The eddy-flux instruments were installed in April of 2001 and measure whole system carbon dioxide exchange between the forest and the atmosphere. The first three transects were set up in the wind “footprint” of the tower, radiating away from the tower in the three dominant wind directions, northeast, east and southeast (Figure 2). The fourth transect runs south to north, intersecting the middle radial transect at 550 meters. The transects were installed for independent ecological measurements of carbon balance comparable to the whole system carbon dioxide measurements from the eddy-flux tower. Each transect measures 1000m by 50m, covers 5 ha, and is organized using an X-Y coordinate system. The X direction runs the length of the transect and starts at 0 m. The Y direction is perpendicular to the centerline with the origin on the centerline. The transect design samples a larger area than “small scattered plots” designs, and the long, thin transects incorporate the spatial variation inherent in tropical forests. The inclusion of the transverse transect tested for directional bias in the forest.

Other research teams have instruments installed on both the tower and the forest floor at the km 67 site measuring general meteorology, atmospheric gas profiles, soil nutrients, soil fluxes and isotopic exchange. Most of the experiments at the km 67 site are replicated at two

Figure 2: Map of Transects and CWD plots for km 67 site in the Tapajos National Forest, Brazil. CWD plots were assigned positions from a randomly generated X coordinate between 0 and 940 meters.



sister sites in the Tapajós forest, km 76 site (pasture) and km 83 site (logged forest). All experiments on these three sites are part of a larger project called the Large-scale Biosphere Atmosphere experiment in Amazonia that has the broad goal of understanding the effects of tropical forest conversion and global climate change on ecosystem function, carbon budgets and regional and global climates.

METHODOLOGY:

Field Methods

In July of 1999 the four permanent transects were installed and the initial biomass survey of ~2600 trees was performed by another member of the research group. Trees larger than 35 cm diameter at breast height (DBH) and located within 25 m of the centerline were tagged, mapped on the X – Y coordinate system and measured for DBH (taken at 1.3 meters). The DBHs were taken by two Brazilian forestry technicians with over 40 years field experience in Amazon forests. Smaller trees, between 10 – 35 cm DBH located within 5 m of the centerline (4 ha in total), were also tagged, mapped and measured. The DBH for buttressed trees was taken just above the point of buttress termination. Vines, moss or insect nests were removed prior to measurement because they can lead to errors in the estimation of DBH. Ten and 35 cm were chosen as the minimum diameters for the two size classes because 10 cm is the most common minimum size for ecological studies and 35 cm is the most common minimum size for logging inventories. A subsampling design was used for 10 – 35 cm trees due to the large number of stems in that size class.

Nelson Rosa, a field botanist from the Museo Gueldi, Belém, collected specimens of each tagged tree and provided botanical identification to species. He was assisted by the two above mentioned forestry technicians.

Of the ~2600 tagged trees in the original survey, 1000 were banded with spring mounted stainless steel dendrometers in December of 1999. Dendrometer measurements are not considered in this thesis, because DBH surveys are used to provide assessments of growth and biomass change. However, a distinction is made between banded and unbanded trees because they were measured separately for DBH in 2001.

In 2001, all permanently tagged trees were re-surveyed to measure carbon flux and changes in the standing stock. In July of 2001 a re-survey of the ~1600 unbanded trees was conducted by the forest technicians, Brazilian students and myself; another member of the research team conducted a re-survey of the ~1000 banded trees in April of 2001 with the technicians and students. All trees in the initial survey were located, the tags and X – Y coordinates were verified, the status (alive/dead/broken/fallen) was recorded and a new DBH was taken by one of the two forestry technicians. In addition, an inventory of previously untagged stems was performed for trees larger than the minimum diameter requirements for each size class. Trees were tagged with a unique number, mapped, measured and identified to common name by the same forestry technicians that assisted with botanical identifications during the original survey. Trees that grew into the 10 cm size class were termed “recruitment”; trees that grew into the 35 cm size class are not considered as “recruitment” because the growth term of the carbon budget accounts for carbon storage in trees > 35 cm.

A biomass inventory of coarse woody debris (CWD) was also performed in 2001. CWD was divided into two different classes: standing CWD and fallen CWD. A network of new subplots within the existing transects (Figure 2) was installed for the measurement of fallen CWD. Three different size classes of wood were measured in three different sized subplots; the plot locations, subplot sizes and subplot design are shown in Figure 2.

A top, middle and bottom diameter was measured for fallen CWD with either a large tree caliper or a small electronic caliper. The length of each piece was measured with a meter tape and all dimensions were recorded. Large and medium pieces were identified to common name by the forest technicians; large pieces were tagged with a unique number and the X - Y co-ordinates of the base were mapped. Only the parts of the wood inside the plot boundaries

were measured and any wood that spanned two adjacent subplots was counted as two separate pieces. Pieces were counted in only one size class; those included in a larger size class were excluded from all smaller size classes.

All pieces of fallen CWD were evaluated for decay class, and all large and medium size pieces were evaluated for biological characteristics, physical characteristics and percentage bark cover. Decay class was determined by correlating external characteristics to density as outlined by Harmon & Sexton (1996) on a scale of 1 to 5:

- Decay class 1 = solid wood, recently fallen, bark and twigs present.
- Decay class 2 = solid wood, significant weathering branches present.
- Decay class 3 = wood not solid, may be sloughing but nail still must be pounded into tree.
- Decay class 4 = wood sloughing and/or friable, nails may be forcibly pushed into log.
- Decay class 5 = wood friable, barely holding shape; nails may be easily pushed into log.

Physical characteristics included the presence of leaves, twigs, branches, bark on branches, bark on bole, sloughing sapwood, friable sapwood, friable heartwood and hollowness. Biological characteristics included presence of conks, moss, lichen, termites and other signs of insects.

Another member of the research group measured standing CWD in April of 2001 in all 20 hectares of forest. All standing trees larger than 10 cm DBH and taller than 1.3 m were included. Each piece was tagged with an original number, identified to common name by the forestry technicians and mapped on the X-Y coordinate system. The DBH was measured and the height was visually estimated to the nearest meter. Decay class was determined using the same criteria as fallen CWD and the following characteristics were used to determine condition of the stem: bole broken; branches present; corrugation; shape of bole; hollow; termites; holes; moss; fungus; totally dead (defined by an absence of sap flow).

Methods for Data Analysis

Three levels of data analysis are performed for above ground biomass on the km 67 site: quantification of carbon pools, characterization of gross and net fluxes, and analysis of

stem/piece dynamics. The total pool is broken up into live biomass and dead biomass and each measured flux and input/output is outlined in Figure 3. All raw data is available on <http://lba-ecology.gsfc.nasa.gov/lbaeco/>.

Live Biomass

Total live biomass for 1999 was calculated from the 1999 DBH inventory. The 2001 live biomass was calculated from the 2001 DBH inventory of banded trees, the 2001 DBH inventory of unbanded trees and the 2001 recruitment survey. Three allometries were used to scale up to biomass from individual DBHs in cm:

Chambers et al. 2001a

$$\text{Kg Biomass} = \exp(-0.37 + 0.333 \cdot \ln(\text{DBH}) + 0.933 \cdot [\ln(\text{DBH})]^2 - 0.122 \cdot \ln[(\text{DBH})]^3)$$

Brown 1997, equation 3.2.3, quadratic

$$\text{Kg Biomass} = 42.69 - 12.800 \cdot \text{DBH} + 1.242 \cdot \text{DBH}^2$$

Brown 1997, equation 3.2.4, exponential

$$\text{Kg Biomass} = \exp(-2.134 + 2.530 \cdot \ln(\text{DBH}))$$

Two of the allometries, the Brown quadratic and the Brown exponential equations (Brown, 1997), were derived from data for tropical forests worldwide including Amazonian, Central American and paleotropical forests, and can be considered generalized estimates. The Chambers equation (Chambers et al., 2001a) was calculated from destructive sampling of 315 trees from a forest in Manaus, a region 370 km west of our site with comparable site conditions, forest structure and species compositions to the Tapajós forest, but with somewhat higher precipitation. All the equations give the oven-dry biomass of the woody parts of the tree, including leaves, twigs and bark. Total live biomass was summed for stems 10 – 35 cm and >35 cm and divided by the sampling area, 4 ha and 20 ha respectively. Kilograms biomass was converted to Mg C ha⁻¹ using the value carbon = 50% of biomass (Brown, 1997).

Some trees were missed during the 1999 DBH survey but were recovered during the 2001 recruitment survey (see Net Flux section for methods of determining missed trees). The

DBHs of missed trees were back-calculated two years using the average annual growth rates for each species for inclusion in the 1999 live biomass survey. The April 2001 DBH measurements from the banded trees were corrected to July 2001 for inclusion with the measurements of unbanded trees. The three months of growth were added using the site average annual growth rate of 0.378 cm yr^{-1} .

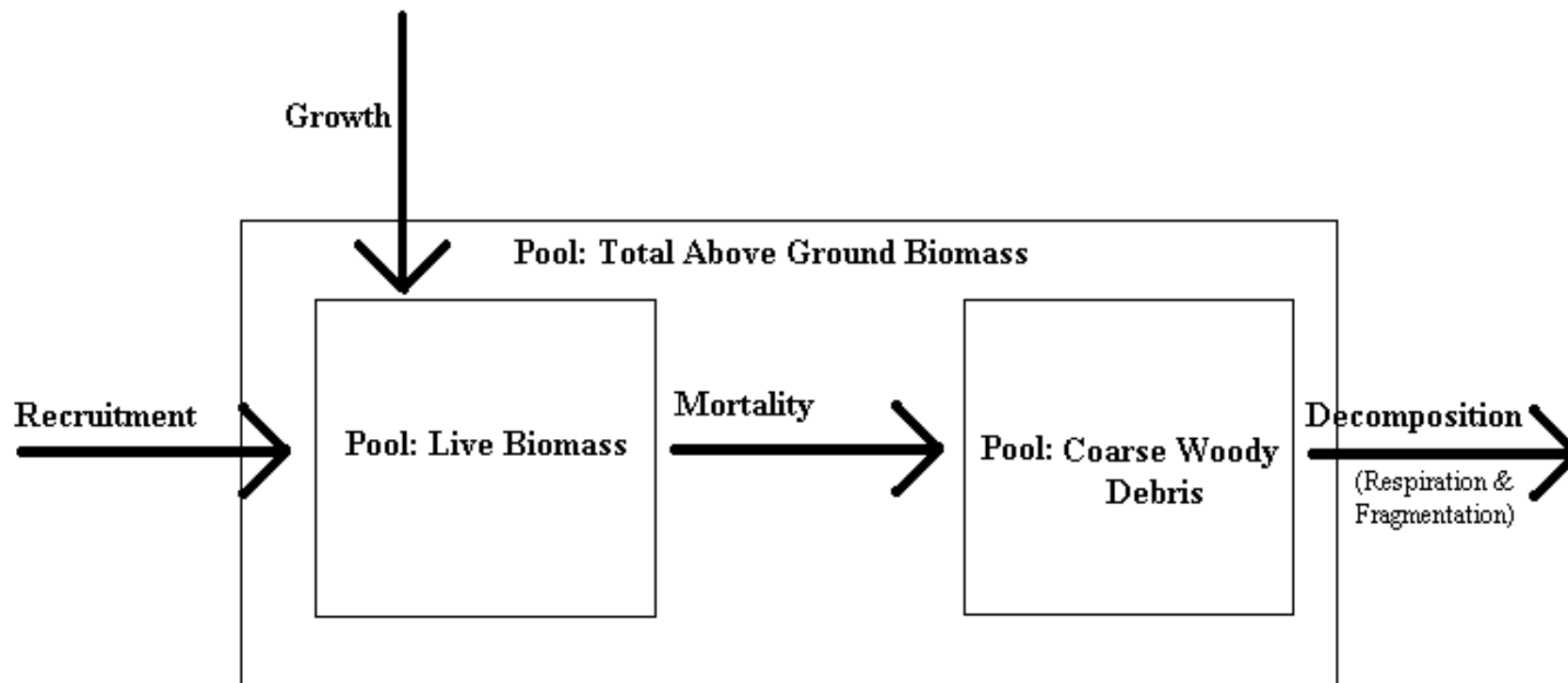
Net Flux in Live Biomass

The total carbon flux in live biomass was calculated by breaking the system down into three carbon flows: growth, recruitment and mortality (Figure 3). Growth was calculated by summing data for all individuals with a DBH measurement in both 1999 and 2001. Recruitment was computed by applying the allometric equations to all stems that grew into the 10 - 35 cm size over the two year period. Mortality was calculated from all tagged individuals that died over the two-year interval. Allometries were applied to the DBH at estimated time of death or the 1999 DBH, whichever was larger. Turnover time of carbon in the live biomass pool was calculated by dividing the total live biomass pool by the gross inputs (growth + recruitment).

In order to exclude outliers in the growth data set caused by measurement error, 66 stems that had growth rates outside of the 5% and 95% confidence intervals, -1 cm yr^{-1} and $+3 \text{ cm yr}^{-1}$, were removed from the growth dataset (Figure 4). The removal of these stems does not change the growth estimate, it only reduces the variance. In order to differentiate missed trees from true recruitment in the 2001 survey of previously untagged trees, average growth rates were calculated for each recruited species and stems that exceeded the average growth rate over the two-year period were removed from the recruitment inventory.

Figure 3: Schematic of carbon cycling in the forest indicating all measured pools, fluxes and flows.

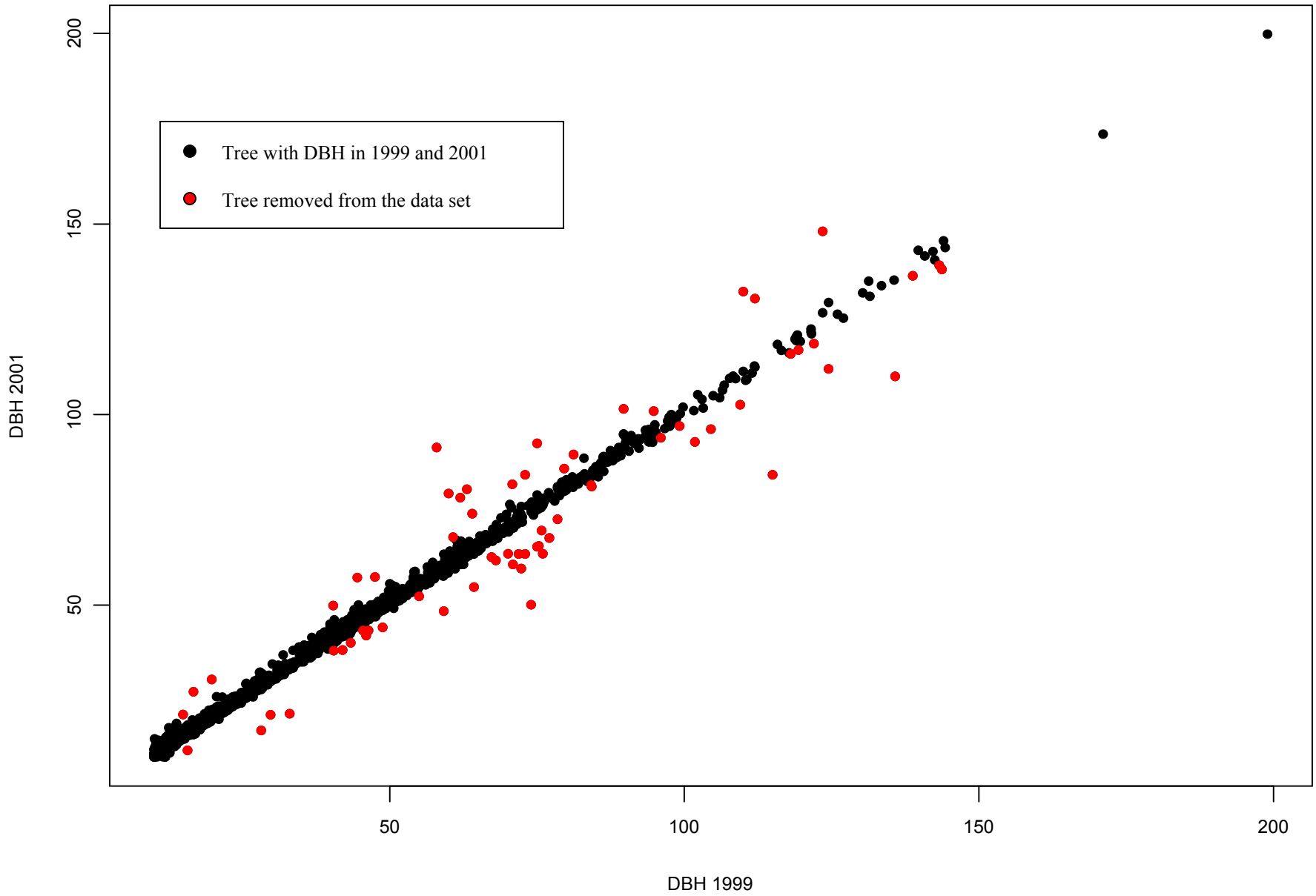
Flux of Carbon in the Forest



Net Flux in Live Biomass:
 $\text{Recruitment} + \text{Growth} - \text{Mortality}$

Net Flux in Dead Biomass:
 $\text{Mortality} - \text{Decomposition}$

Figure 4: Scatter plot of all trees with a DBH in 1999 and 2001 used to create the growth data set. Points in red show the trees that were removed from the growth data set because their growth rates fell outside the 95% range of growth mean (-1, +3 cm DBH yr⁻¹).



Forest Dynamics

The forest dynamics evaluation encompassed a range of different investigations including: difference in biomass and frequency distribution, net flux distribution, growth and biomass increment distributions, mode of death analysis and dynamics of species and functional types.

The change in biomass and frequency distributions from 1999 to 2001 were calculated by binning all of the trees into 35-cm size classes, summing the biomass or frequency per hectare and subtracting 1999 values from the 2001 values. The biomass distribution for the net flux was calculated in a similar manner; carbon in each of the gross fluxes was binned into 35-cm size classes and summed per hectare. Growth increment and biomass increment were evaluated by binning the trees into 5 cm size classes according to 1999 DBH, summing the total increment per size and dividing by the number of trees. Mode of death in mortality was evaluated by separating the trees into the 10 – 35 and the >35 cm size classes and evaluating the percentage of trees that died standing or fallen. Functional type dynamics were evaluated by comparing the percentage of each type in recruitment, mortality and standing stock in 5-cm bins. Recruited trees were assigned functional group classifications by correlating species to potential crown heights as reported in Parotta et al. (1995). Species evaluations were performed by creating sub-samples of the 1999 and 2001 DBH surveys for the five most numerous tree species, binning the sub-samples into 5-cm size classes and summing the frequency per hectare in each year.

Dead Biomass

The total carbon in the dead biomass or CWD pool was calculated by adding together the biomass in fallen CWD and standing CWD. Standing CWD had two size classes: > 30 cm

and 10 – 30 cm. Fallen CWD had three size classes: >30 cm, 10 – 30 cm and 2-10 cm. The 2 – 10 cm size class was included to account for the carbon in fine twigs and branches that are integrated into the allometries for live biomass. To calculate volume for fallen CWD the top, middle and bottom diameters were converted to disk areas and applied to Newton’s Formula (Harmon & Sexton, 1996) for a cylinder:

$$\text{Volume} = \text{length} * (\text{basal area} + 4 * \text{middle area} + \text{top area}) / 6$$

For standing CWD, first the top diameter was calculated using the following formula (Chambers et al., 2000):

$$\text{Top Diameter} = 1.59 * \text{DBH} * (\text{length}^{-0.091})$$

Then, the DBH and top diameter were converted to areas of circles and used to calculate the volume of a snag using an equation for a frustum of a cone (Harmon & Sexton, 1996):

$$\text{Volume} = \text{length} * (\text{basal area} + \sqrt{(\text{basal area} * \text{top area}) + \text{top area}}) / 3$$

CWD volume was converted to biomass by multiplying according to the published density values below:

Published Densities in g cm ⁻³				
<i>Author</i>	<i>Location</i>	<i>Sound</i>	<i>Intermediate</i>	<i>Decayed</i>
Clark et al. (MS)	La Selva, Costa Rica	0.45	0.35	0.25
Delaney et al. (1998)	Venezuelan Amazon	0.50	0.51	0.30
Summers (1998) ¹	Manaus, Brazil	0.46	0.46	0.46

¹ density reported as a single average value for all decay classes of wood.

Clark et al. (MS) and Delaney et al. (1998) used a three class decay system (sound, intermediate, decayed) and Summers (1998) reported a single average density. The five-class decay system used for field measurement was converted to the three-class system as follows: decay 1 – 2 became the sound class; 2.5 –3.5 became the intermediate class; and 4-5 became the decayed class.

Net Flux in Dead Biomass

The total carbon flux in CWD was calculated by breaking the system down into inputs from mortality and subtracting outflows from decomposition (see Live Flux section for methods of mortality calculation). Decomposition represents both respiration and fragmentation from all CWD and was calculated by multiplying the total CWD pool by one of two published k constants: $k = 0.17 \text{ yr}^{-1}$ (Chambers et al., 2000) or $k = 0.15 \text{ yr}^{-1}$ (Summers, 1998). The k constants represent a constant fraction of mass lost over time (t) and were determined from change in CWD mass over several years in two terra firme forests in Manaus. Turnover time of carbon in CWD was calculated by dividing the total CWD pool by the input to CWD from mortality for comparison with the residence time ($= 1/k$).

Uncertainty

Uncertainty was calculated for all gross fluxes, net fluxes and pools by bootstrapping the existing datasets. Calculated uncertainties cover estimates of sampling and measurement uncertainties only and do not attempt to quantify other sources of uncertainty (e.g. allometric errors). One thousand random samples were drawn with replacement from each existing dataset with the same number of individuals (n). Uncertainty was reported as the difference between the 5% or 95% confidence interval and the reported mean; the largest difference was selected as the uncertainty estimate calculated for each recruited species and stems that exceeded the average growth rate over the two-year period were removed from the recruitment inventory.

RESULTS:

Live Biomass

The live biomass estimate, derived from a total of 1791 trees surveyed in 2001, ranged from $145.5 \pm 4.9 \text{ Mg C ha}^{-1}$ to $159.7 \pm 9.2 \text{ Mg C ha}^{-1}$ depending on allometry (Table 1). The $\pm x$ values denote the 95% confidence intervals for sampling variation and do not include estimates of allometric errors. The sampling error was very small and indicates that the sample was robust and the size of the sample did not affect the accuracy of the estimate.

The 2001 stem frequency diagram (Figure 5) shows a large number of trees/ha in the small size classes and decreasing numbers in the medium and large sizes; roughly half of the trees are smaller than 20 cm DBH. Stem density quickly dwindles due to the self-thinning effect in population dynamics and because many trees reach maturity at small sizes. This produces the expected “reverse J-shaped” stem frequency distribution (Brown, 1997). In contrast, carbon distribution is more evenly spread out and decreases in a roughly linear fashion over the size classes (Figure 5). The contribution of carbon from large trees is disproportionate to their numbers: trees greater than >35 cm contain 66% of biomass but constitute only 36% of stems. As a result, the live biomass estimate is greatly influenced by the contribution of a relatively small number of large trees.

Net Flux in Live Biomass

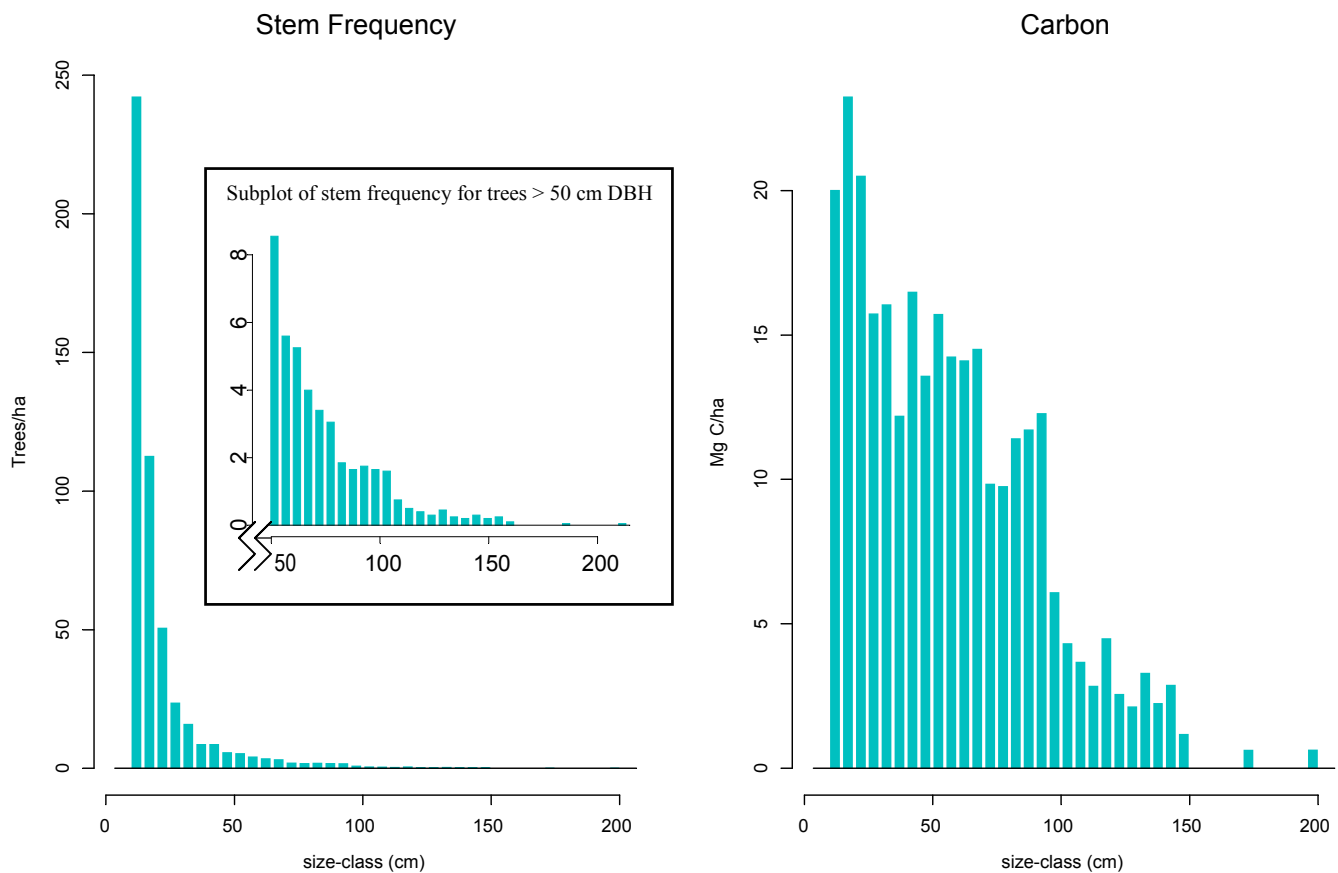
Net flux of carbon in live biomass is determined by adding together the inflow of carbon from growth and recruitment and subtracting the outflow of carbon from mortality (Table 2). Carbon inflow totaled $3.63 \text{ Mg C ha}^{-1} \text{ yr}^{-1}$ with $0.40 \pm 0.01 \text{ Mg C ha}^{-1} \text{ yr}^{-1}$ from recruitment and

Table 1: Pool of Carbon (Mg C ha⁻¹) in living biomass greater than 10 cm DBH

Pool: Living Biomass			
year	Allometry 1 ^a	Allometry 2 ^b	Allometry 3 ^c
1999 (n= 2731)	144.1 (±4.9)	154.4 (±7.8)	161.0 (±9.3)
2001 (n=2791)	145.5 (±4.9)	154.5 (±6.9)	159.7 (±9.2)
-----	-----	-----	-----
Difference yr ⁻¹	0.7 (±8.2)	0.1 (±11.24)	-0.7 (±14.7)

^a from Chambers *et al.*, 2000; ^b from Brown, 1997, equation 3.2.3; ^c from Brown, 1997, equation 3.2.4

Figure 5: distributions of stem frequency and carbon in 2001



$3.23 \pm 0.18 \text{ Mg C ha}^{-1} \text{ yr}^{-1}$ from growth; outflow from mortality was $-3.13 \pm 0.57 \text{ Mg C ha}^{-1} \text{ yr}^{-1}$ (see Table 2 for range by allometry).

The net flux, computed from carbon inflow and carbon outflow to the pool, ranges from $0.50 \pm 0.88 \text{ Mg C ha}^{-1} \text{ yr}^{-1}$ to $-0.78 \pm 1.91 \text{ Mg C ha}^{-1} \text{ yr}^{-1}$ depending on allometry. The annualized difference in the standing stock of live biomass from 1999 to 2001 ranges between $0.7 \pm 8.2 \text{ Mg C ha}^{-1} \text{ yr}^{-1}$ and $-0.7 \pm 14.7 \text{ Mg C ha}^{-1} \text{ yr}^{-1}$. Both methods should and do produce roughly the same range of estimates because they measure the same phenomenon (change in carbon pool) by different methods. However, the net flux method has a much smaller uncertainty because tracking individual trees to determine carbon change is a superior method to observing aggregate changes between two biomass inventories (Clark et al., 2001). The range of net live flux estimates and the changes in standing stock all encompass zero; thus, there is no measurable storage or release of carbon from live biomass. The full range of live flux estimates from $+1.38 \text{ Mg C ha}^{-1} \text{ yr}^{-1}$ (carbon gain) to $-2.69 \text{ Mg C ha}^{-1} \text{ yr}^{-1}$ (carbon loss) indicates that there is, at most, a small change in live carbon stocks over this two year interval.

Dynamics in Recruitment, Growth and Mortality

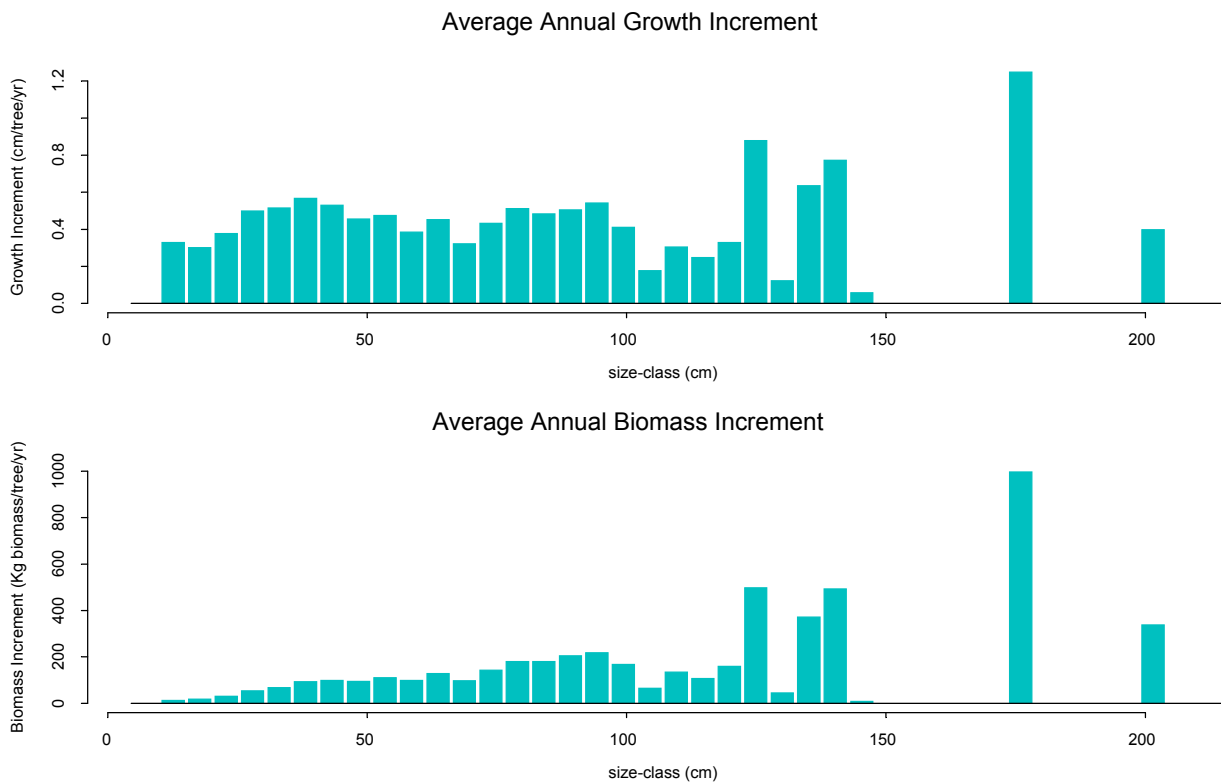
Recruitment was determined from 189 trees that grew larger than the 10-cm minimum over the two-year period. These stems had an average basal area of $0.22 \text{ m}^2 \text{ ha}^{-1}$ and a frequency of 24 stems ha^{-1} . Recruitment amounted to 0.27 % of 2001 biomass and growth amounted to 2.2%. A comparison of pool size to inputs ($145.5 \text{ Mg C ha}^{-1} / 3.63 \text{ Mg C ha}^{-1} \text{ yr}^{-1}$) translates to a carbon turnover time of ~40 years in the live biomass pool. For trees 10 – 35 cm the ratio ($49.6 \text{ Mg C ha}^{-1} \text{ yr}^{-1} / 2.6 \text{ Mg C ha}^{-1}$) translates to a turnover time of ~19 years, and for trees > 35 cm the ratio ($95.9 \text{ Mg C ha}^{-1} \text{ yr}^{-1} / 1.0 \text{ Mg C ha}^{-1}$) translates to a turnover rate of ~96 years. Turnover time is shortest for small stems because the pool is more labile with frequent stem replacement

Table 2: Flux of carbon (MgC/ ha/yr) in living biomass greater than 10 cm DBH. Carbon numbers are reported for three allometries used to scale DBHs to biomass.

<u>Flux: Living Biomass</u>			
<u>Flow</u>	Allometry 1 ^a	Allometry 2 ^b	Allometry 3 ^c
Inflow: Recruitment	0.40 (± 0.01)	0.34 (± 0.01)	0.34 (± 0.01)
Inflow: Growth (DBH comparison)	3.23 (± 0.18)	3.34 (± 0.19)	3.25 (± 0.21)
Outflow: Mortality	3.13 (± 0.57)	3.81 (± 1.20)	4.37 (± 1.68)
-----	-----	-----	-----
Total	0.50 (± 0.88)	-0.13 (± 1.24)	-0.78 (± 1.91)

^a from Chambers *et al.*, 2000; ^b from Brown, 1997, equation 3.2.3; ^c from Brown, 1997, equation 3.2.4

Figure 6: Comparison of annual growth increment and annual carbon increment.



and because it takes a longer period of time to reach a large DBH. Nevertheless, turnover times for the big trees are still rapid relative to temperate and boreal forests (Malhi et al., 1999). The large size of the standing stock and the short turn over time indicates that there is a great deal of carbon movement within the live biomass pool and that the Tapajós forest annually cycles a large mass of carbon.

The annual growth increment in DBH is roughly the same for all size classes (Figure 6), while biomass increment increases with tree size. The different effects of size class on growth and biomass increment result from the power series relationship between biomass and DBH and explain why the frequency distribution of standing stock declines with DBH while the relative importance of biomass increases with DBH (Figure 5).

Mortality was quantified from 98 trees that died between 1999 and 2001; their basal area was $0.61 \text{ m}^3 \text{ ha}^{-1}$. The annualized mortality rate was 1.8 % of the standing stock and the stem turnover rate is ~57 years (calculated from the ratio of stems in standing stock to stems in annual mortality, 2791:49). Standing stock mortality rates were not constant over all size classes (Figure 7); percent mortality increases with DBH. Trees $> 70 \text{ cm DBH}$ had an average mortality of 3.7% while trees $< 70 \text{ cm DBH}$ have an average mortality of 1.6%. In a steady-state forest, percent mortality should be relatively even over all size classes such that demographic structure of the forest is maintained. However, in the Tapajós National Forest this is not the case because a greater percentage of large trees are dying (Figure 7).

In addition, the mode of death is not the same for all size classes. Of the trees that died, 61% of stems died standing and 39% of stems died when they fell over or were broken. However, in the small and large size classes, there was a marked difference in the percent of trees that died falling/breaking and trees that died standing (Figure 8). Small stems were more

Figure 7: Annual percent mortality of the standing stock by size class.

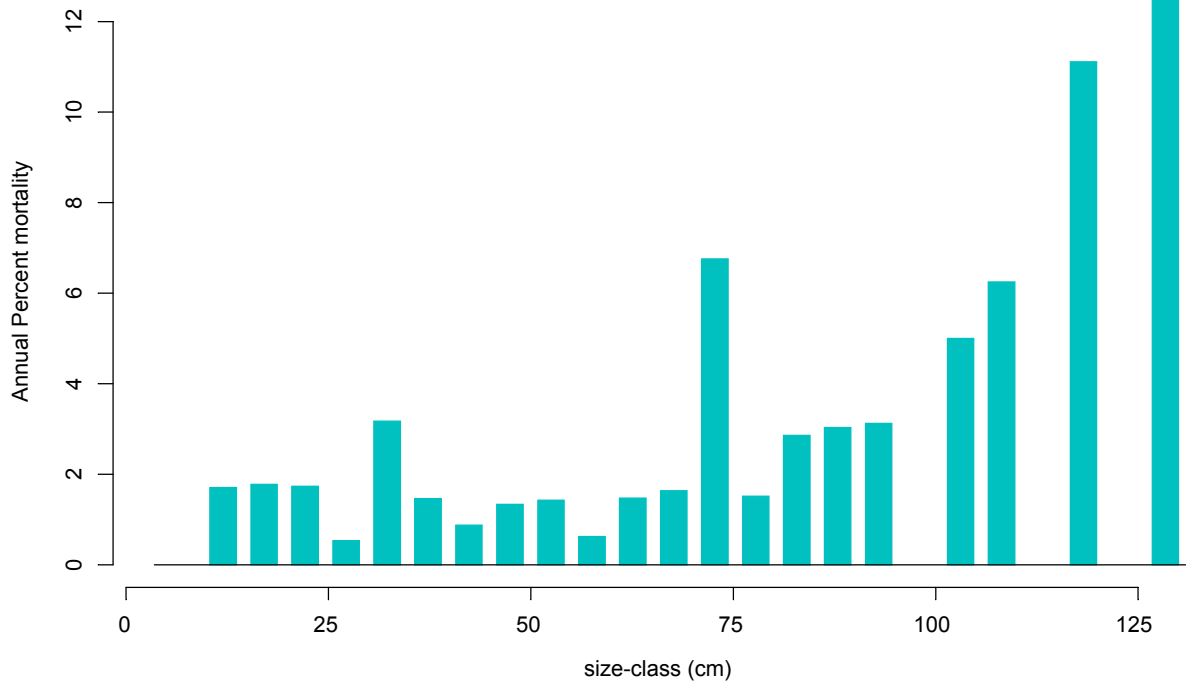
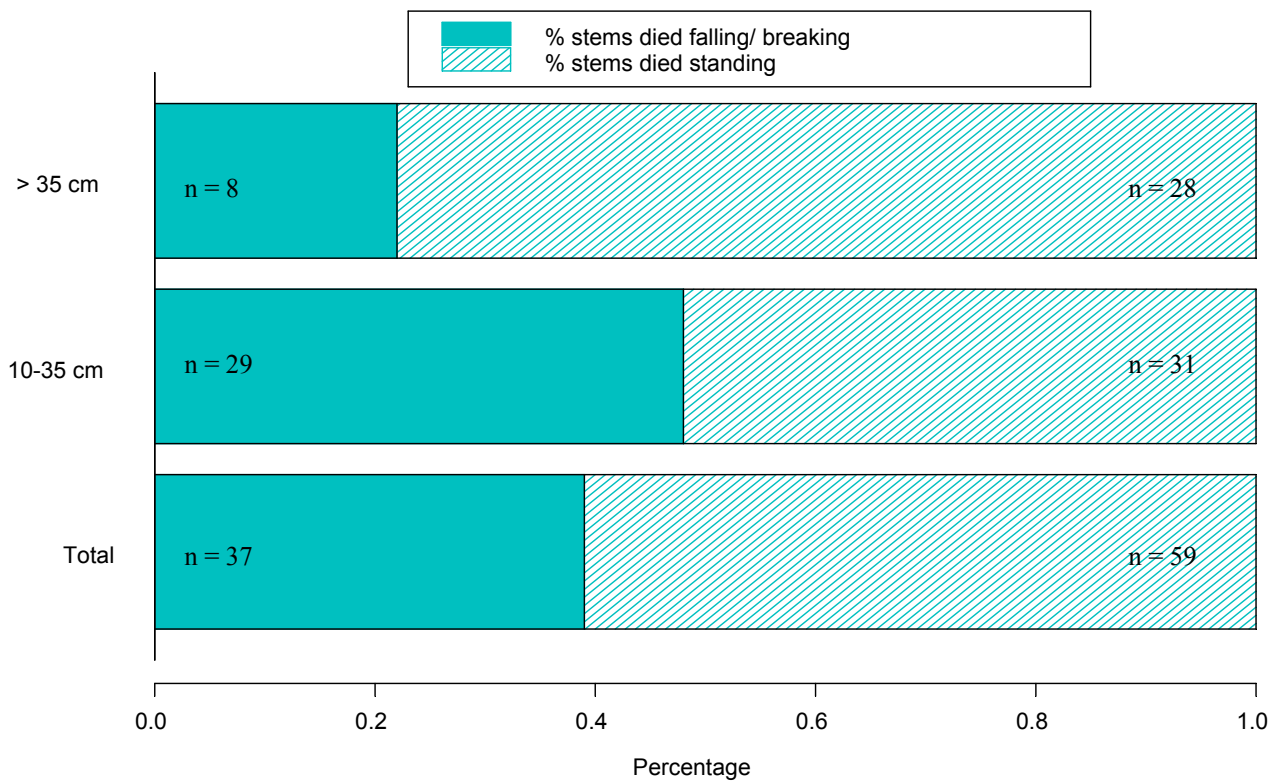


Figure 8: Comparison of numbers of trees that died standing and trees that died falling for mortality between 1999 and 2001 (numbers not annualized).



likely to die by falling or breaking than large stems, which suggests that causes of mortality differ as a function of stem size. The larger trees probably die from water stress, pests or senescence while understory trees may be more susceptible to wind throw or breakage during treefalls.

Forest Dynamics

Analysis of forest dynamics provides context for the carbon budget because changes in demographic patterns can affect the carbon flux. Dynamics were evaluated in four different ways: (1) differences between 1999 and 2001 DBH surveys (Figure 9); (2) variation in live carbon flux by size class (Figure 10); (3) forest functional group dynamics (Figure 11; Figure 12) and (4) distributions of the five dominant species (Figure 13).

The distributions of stem frequency and DBH differences between 1999 and 2001 (Figure 9) reveal several key changes in standing stock. There were more trees present in the size classes < 60 cm than there were in the large size classes (Figure 9a). The same trend was present in biomass change with $2.9 \text{ Mg C ha}^{-1} \text{ yr}^{-1}$ accumulated in classes < 60 cm but $-2.2 \text{ Mg C ha}^{-1} \text{ yr}^{-1}$ dispersed from the size classes > 60 cm (Figure 9b). The loss of carbon and the decreased stem frequency in the larger size classes is consistent with the high mortality rates observed in these size classes (Figure 7). Taken together, these two graphs suggest that there may have been a demographic shift towards smaller stems and consequently increased biomass in the <60 cm size classes over this two year period.

Similar to the earlier comparison of total change in biomass surveys (Table 1) to net live flux (Table 2), changes in carbon distribution across size classes (Figure 9b; Figure 10) can be compared meaningfully because both figures measure changes in carbon but through different methods. Each method estimates similar carbon balances for each size class but carbon flux data

Figure 9: Difference in stem frequency and in carbon between 1999 and 2001.

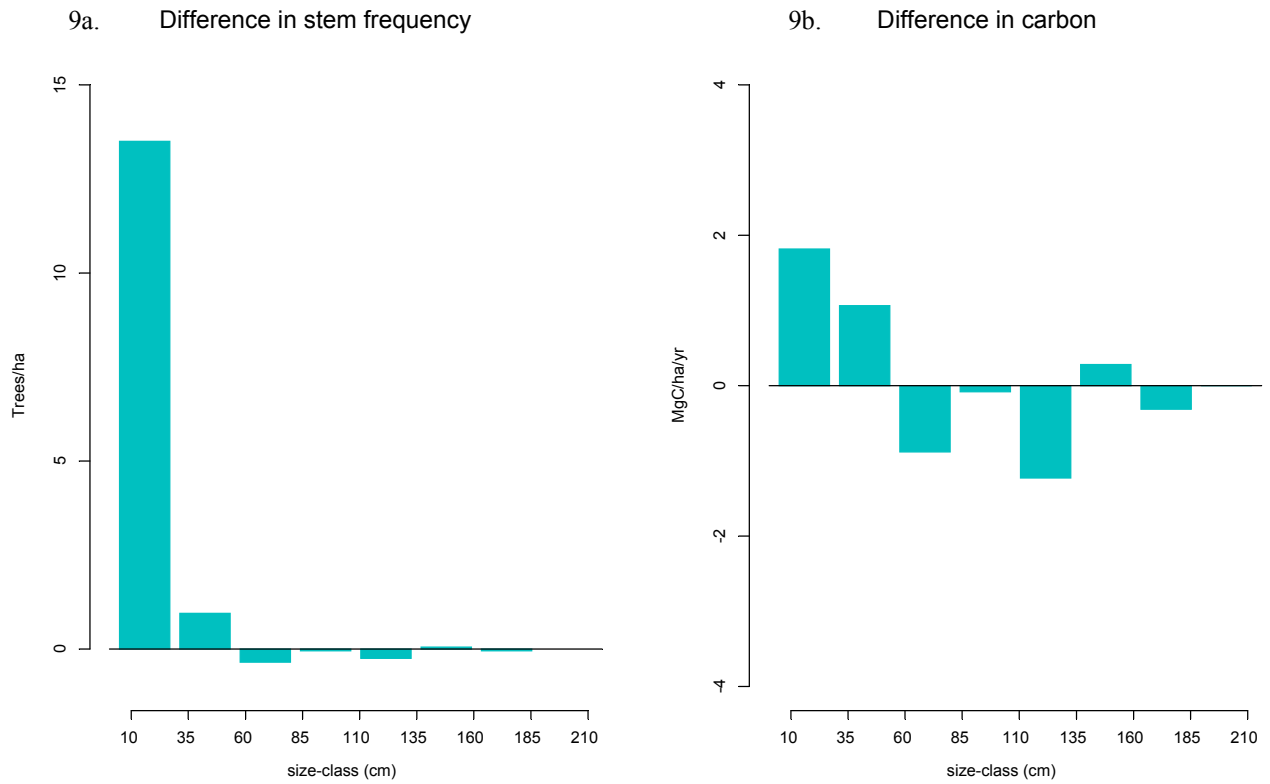
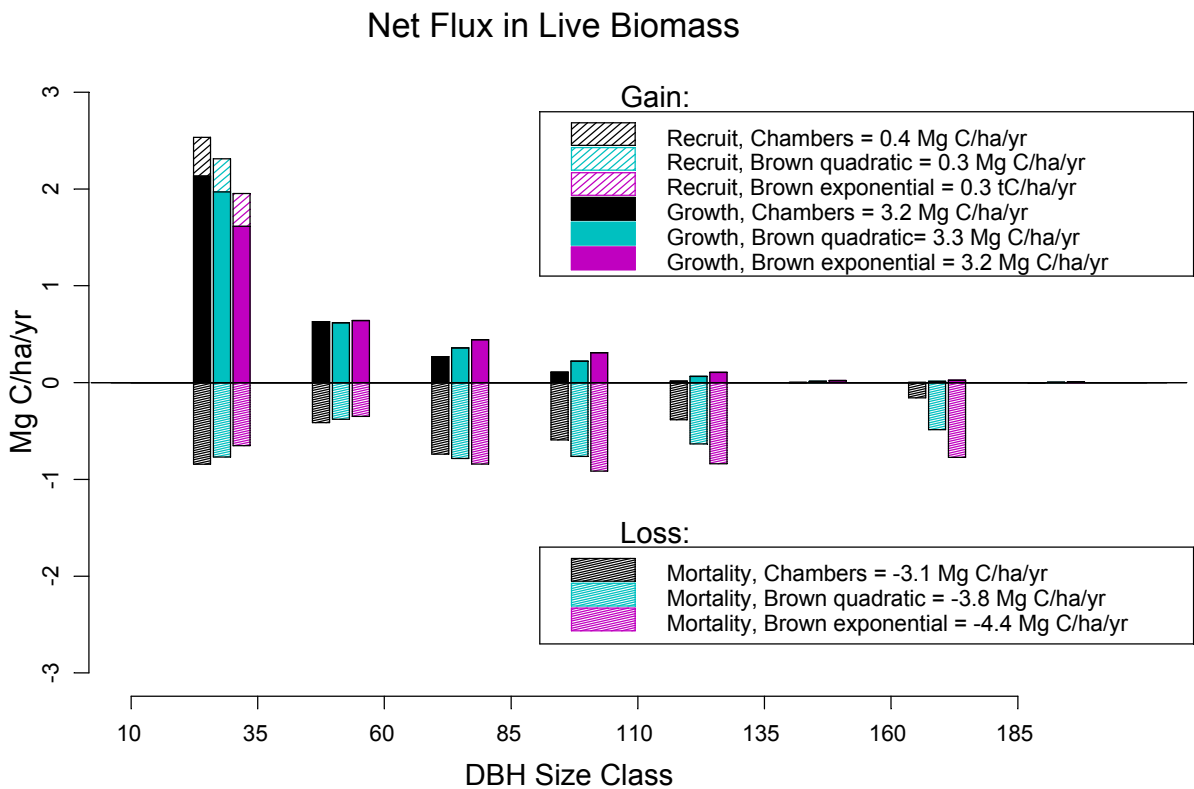


Figure 10: The net flux of carbon in live biomass pool



are broken into individual inputs and outputs of carbon (Figure 10). Net carbon storage in small size classes is balanced by net carbon release in large size classes, leaving the total flux for live biomass (Table 2) roughly in carbon equilibrium. Recruitment and growth are skewed toward more carbon accumulation in small size classes and less carbon accumulation in large classes. The high growth rates in the smaller size classes could represent a possible response to better light conditions resulting from the high mortality observed in large trees (Figure 7).

In contrast to growth and recruitment, mortality has an approximately even distribution of carbon loss throughout the entire standing stock. However, the mortality skews carbon release towards the larger sizes because there is no accretion to offset loss. Finding an even distribution of carbon loss from mortality is unusual because the biomass distribution in live trees decreases with size (Figure 5). Thus, from the perspective of the carbon budget, a roughly even distribution of carbon loss from mortality represents an unusually high amount of carbon loss from the largest size classes.

Two size classes, 60 – 85 cm and the > 110 cm, are responsible for the majority of carbon loss and frequency decline contributing -0.88 and -1.26 Mg C ha⁻¹ respectively (Figure 9b). In the 60 – 85 cm size class, 54 % of the trees that died were canopy species and 46% were emergent species, while all of the >110 cm trees that died were emergents. Because emergent species grow taller than canopy trees, they constitute a larger percentage of the standing stock in very large size classes. In the 60 – 85 cm size class, one quarter of the trees died falling/breaking while 100% of trees in the larger size class died standing (6 of 6). This is consistent with the observation that larger trees are more likely to die upright (Figure 8). Because the trees responsible for the carbon loss in largest size classes generally died standing, their mortality seems to be associated with tree health as opposed to wind disturbance.

The relative percentages of the four functional types (emergent, canopy, subcanopy, pioneer), that were derived by correlating species identifications to potential crown heights, were compared between recruitment, mortality and standing stock (Figure 11). The relative percentages of functional types in the different standing stock size classes matches the life strategy of each group. Subcanopy trees make up a large percentage of the small size classes but taper out quickly with size; emergent trees are a very minor percentage of stems at small size but have rising prominence as DBH increases. Canopy trees gain importance in the middle size classes but have decreased presence in the large and small classes; pioneers have a small but almost constant representation in standing stock up to 70 cm DBH.

The functional type growth increment by size class (Figure 12) shows that each functional type has a growth strategy that corresponds to its light conditions and potential crown height in the forest. Subcanopy growth peaks in the smallest size classes and declines after 35 cm when subcanopy trees start to senesce. Emergent growth is highest after 60 cm DBH when the trees have probably reached canopy height and higher light conditions. The growth rates of canopy trees are strongest between 35 and 85 cm DBH, indicating that they have maximal growth after they break out of the shaded understory. Pioneer growth rates are much larger than other groups and peak around 35 cm DBH, corresponding with colonization of open conditions. However, their intrinsically high growth rates mean that they cannot survive outside of gaps. Mean growth rates (DBH) reflect the average available light conditions for each functional group and are listed in ascending order: subcanopy (0.27 cm/yr), canopy (0.41 cm/yr), emergent (0.45 cm/yr), pioneer (0.56 cm/yr).

Comparison of recruitment and mortality by functional group offers a potential mechanism for the demographic changes noted in figures 9 & 10. Recruitment and mortality

Figure 11: Contribution to recruitment, mortality and standing stock by functional type

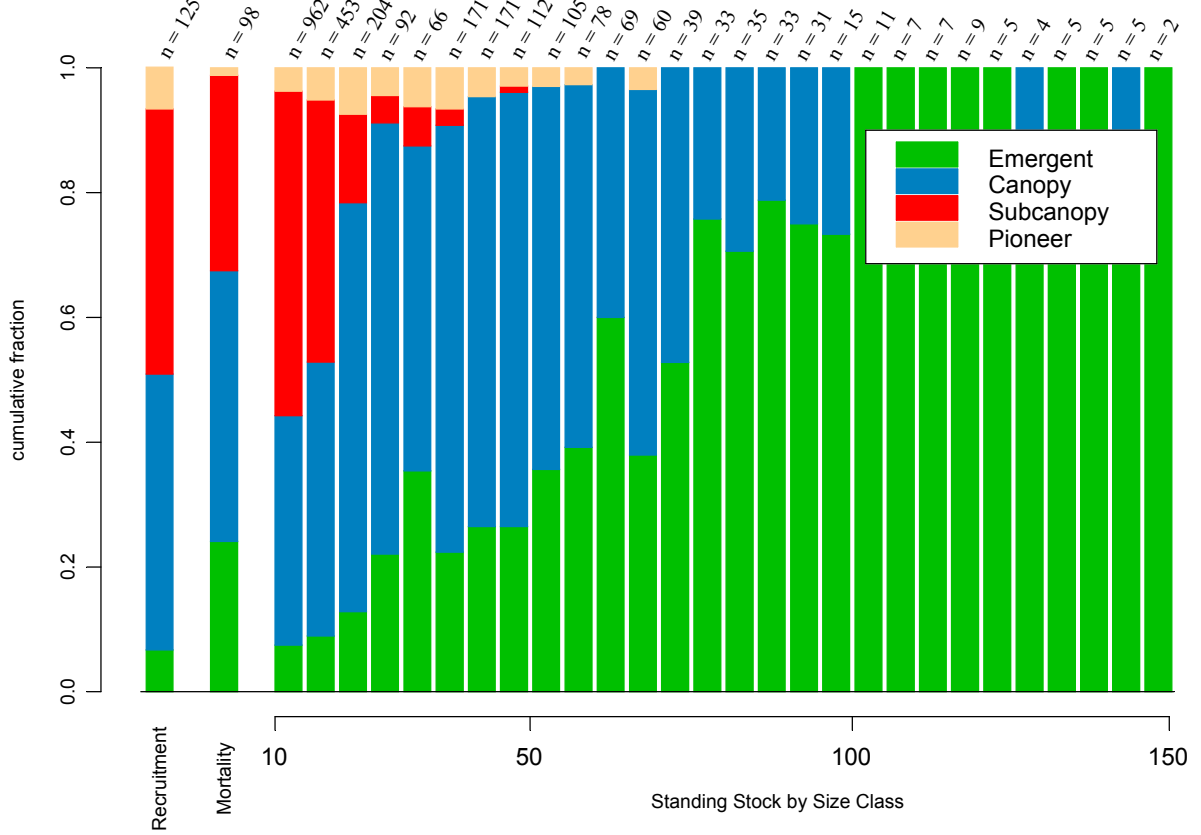
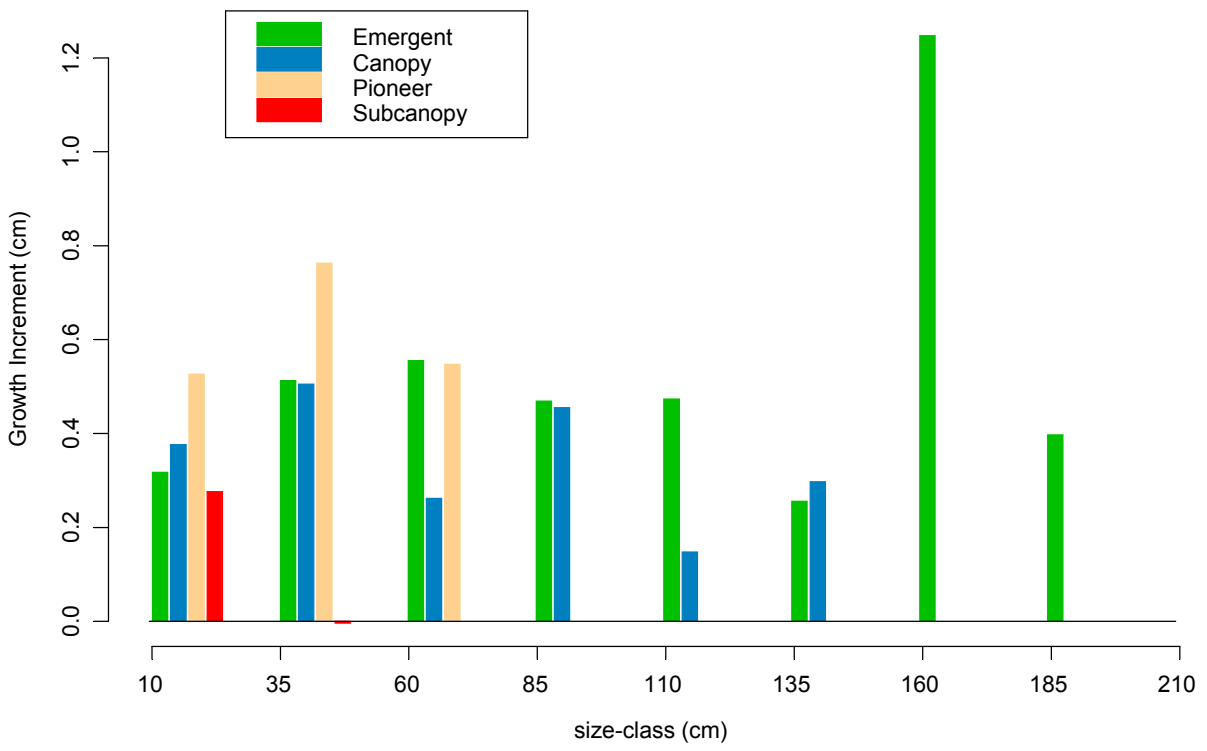


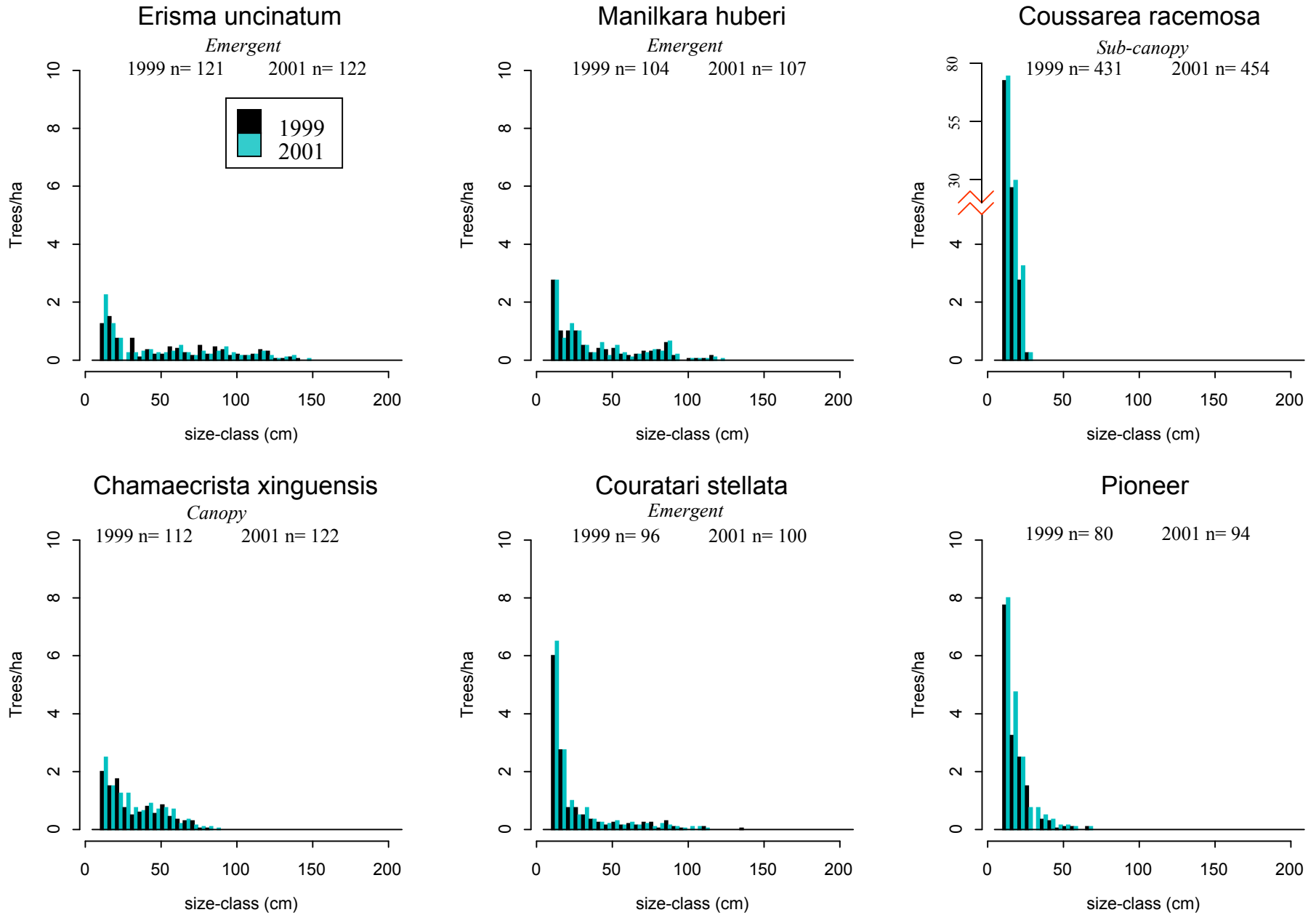
Figure 12: growth increment by functional type



represent the inflow and outflow of stems to the standing stock. Thus, the two flows should have roughly equal proportions of functional types for a steady state forest over the long term. In this case, however, recruitment has a greater percentage of subcanopy and pioneers and a much smaller percentage of emergents compared to mortality. The prominence of emergents in mortality suggest that there was episodic death of some very large trees (> 60 cm DBH). This concurs with the earlier observation that the mortality rates were disproportionately high in the large size classes. As previously stated, the mortality rate in trees > 70 cm DBH is 3.7%, more than twice the site average mortality rate of 1.8%. In addition, the mortality rate for trees > 70 cm DBH is significantly larger than any other published mortality rate for the neotropics (Swaine et al., 1987; Phillips & Gentry, 1994) which range between 0.46% (Swaine et al., 1987) and 3.08% (Phillips & Gentry, 1994). The death of an emergent creates a large gap that is likely to be filled with many pioneers and subcanopy species. Our study documents both the increased number of small trees (Figure 9a) and death of very large trees (Figure 9a). Thus, a pulse of mortality in very large trees and subsequent canopy gaps could be the mechanism behind the demographic changes.

An examination of individual species corroborates the demographic shift noted in Figures 9 & 10 and the increased percentage of recruited subcanopy and pioneer species in Figure 11. Figure 13 evaluates the size distributions of the five most common species and the pioneer functional type in 1999 and 2001. Four of the species, *Erisma uncinatum*, *Chamaecrista xinguensis*, *Manilkara huberi* and *Couratari stellata*, have similar distributions in both years. However, *Coussarea racemosa*, an understory species and the pioneer group, have more trees per hectare in the three smallest size classes in 2001. *Coussarea racemosa* alone constitutes 50% of the subcanopy recruitment but it is not recruiting in proportion to its 75% presence of all

Figure 13: A comparison of stem density in 1999 and 2001 in the five most common species and the pioneer functional group



subcanopy stems. Therefore, *Coussarea racemosa* is not solely responsible for the demographic shift and the increase in subcanopy tree dominance. Other, less common subcanopy species such as *Aparisthium cordatum* and *Poecilanthe effusa* are also likely contributors to these phenomena.

Dead Biomass

A total of 830 pieces of fallen CWD and 560 stems of standing CWD were measured resulting in an average volume of $198.6 \pm 17.5 \text{ m}^3 \text{ ha}^{-1}$ (Table 3). Because site-specific wood density numbers were not available, a range of pool estimates was reported for dead biomass based on different published densities. CWD is broken down into two components: fallen and standing. Fallen wood had an average volume of $154.0 (\pm 16.9) \text{ m}^3 \text{ ha}^{-1}$ and covered an average area on the forest floor of $28.7 \text{ m}^2 \text{ ha}^{-1}$ (calculated from the square of the inverse cubed root of volume). Standing wood had an average volume of $36.6 \pm 6.3 \text{ m}^3 \text{ ha}^{-1}$ and a stem density of 28 stems ha^{-1} . Sampling uncertainties for both fallen and standing CWD were greater than 10% and the standing CWD uncertainty is about 5% larger than the fallen CWD uncertainty. Sampling accuracy of the CWD estimate may be improved with larger and more numerous plots for both fallen and standing CWD.

Fallen wood constitutes about 81% of the dead volume and standing wood constitutes only 19%. In contrast, 40% of stems die falling while 60% of stems die standing (Figure 8). Although a greater number of trees die upright, trees topple as they decay and consequently there is more dead wood in fallen CWD at any given time.

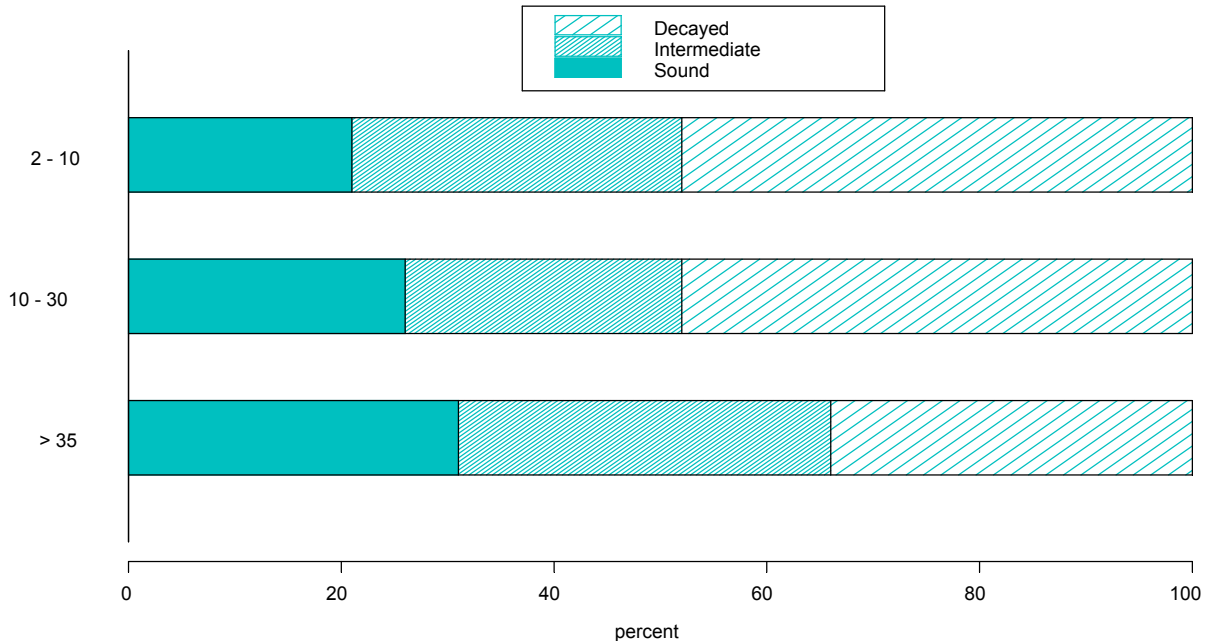
The fallen CWD plots were highly variable; there was a 6-fold variation of volume among the $> 30 \text{ cm DBH}$ plots and a 13-fold variation of volume amongst the $10 - 30 \text{ cm DBH}$

Table 3: Pool of carbon (MgC/ ha) and volume (m3/ ha) in coarse woody debris at km 67, Tapajós National Forest, Brazil. Numbers are reported from published three density groups systems used to convert volume measurements to biomass.

<u>Fallen Coarse Woody Debris</u>				
<u>size</u>	Volume	Density group 1 ^a	Density group 2 ^b	Density group 3 ^c
>30cm (n=246)	97.9	17.1	21.6	22.5
10 - 30cm (n=194)	36.8	6.2	7.7	8.5
2 - 10cm (n=390)	19.3	3.2	4.0	4.5
-----	-----	-----	-----	-----
Fallen subtotal (n=830)	154.0 (± 16.9)	26.5 (± 2.8)	33.3 (± 3.9)	35.4 (± 3.7)
<u>Standing Coarse Woody Debris</u>				
<u>size</u>	Volume	Density group 1	Density group 2	Density group 3
>30cm (n=220)	33.9	5.7	7.5	7.8
10 - 30cm (n=340)	2.8	0.4	0.6	0.6
-----	-----	-----	-----	-----
Standing subtotal (n=560)	36.6 (± 6.3)	6.2 (± 1.1)	8.1 (± 1.6)	8.4 (± 1.4)
<u>All Coarse Woody Debris</u>				
<u>size</u>	Volume	Density group 1	Density group 2	Density group 3
>30cm (n=466)	131.7	22.8	29.1	30.3
10 - 30cm (n=534)	47.6	6.6	8.3	9.1
2 - 10cm (n=390)	19.3	3.2	4.0	4.4
-----	-----	-----	-----	-----
Total (n=1390)	198.6 (± 17.5)	32.6 (± 2.9)	41.4 (± 4.1)	43.8 (± 4.1)

^a from Clark *et al.*, MS; ^b from Delaney *et al.*, 1998; ^c from Summers, 1998

Figure 14: Percent of Fallen CWD piece by decay class



plots. However, there was no spatial pattern correlated with the amount of CWD. The plot variation is best explained by the spatial and temporal variation of mortality. In addition, CWD had a similar distribution of species to the standing stock of live trees. This indicates that no single species was favored or eliminated in a past mortality event. The five most common species in the > 30 cm dead wood, *Sclerolobium spp.*, *Sapotaceae burseraceae*, *Erismia uncinatum*, *Pseudopiptadenia psilostachya* and *Chamaecrista xinguensis*, were among the 10 most common species for trees > 30 cm DBH.

The number of CWD pieces in each decay class differs with size and there is significantly more decayed wood in the 2 – 10 cm and 10 – 30 cm size class than > 30 cm size class (Figure 14). Three processes can explain this difference: fragmentation, volume loss and increasing decay rate. As wood decays, it decreases in volume and breaks up into smaller fragments, which increase the available surface area for active microbial decay. This accelerates the decomposition process. There is more decayed wood than sound wood in terms of volume: 36% of CWD volume is in decayed wood, 34% in intermediate and 30% in sound. However, there is proportionally more carbon in sound wood: 40% of carbon is in sound wood, 34% in intermediate and only 26% in decayed (using Clark et al. (MS) densities). This disparity reflects declining wood density during decomposition. In contrast to our findings, 89% of mass in CWD was in the sound class alone for a forest in La Selva, Costa Rica (Clark et al., MS), indicating that either the decay class system differed from Clark et al. (MS) or that there were different input rates, decay mechanisms, or time periods for measurements in La Selva, Costa Rica and the Tapajós.

Net Flux in Dead Biomass

Net flux in dead biomass is calculated by subtracting the computed carbon outflow (wood decomposition) from the carbon inflow (mortality). The inflow, or mortality in tagged trees since the 1999 survey, totals $3.1 \pm 0.6 \text{ Mg C ha}^{-1} \text{ yr}^{-1}$ while the outflow attributed to decomposition is between 4.9 ± 0.5 to $7.5 \pm 0.7 \text{ Mg C ha}^{-1} \text{ yr}^{-1}$, depending on the densities used to calculate carbon content and on the decomposition rate. Thus, net flux in dead biomass ranges between -0.5 to $-4.4 \text{ Mg C ha}^{-1} \text{ yr}^{-1}$ (Table 4). The range of net flux is negative and indicates steady state or a small decline in the pool size.

The small decrease in the CWD pool suggests that the measured mortality inputs to the CWD pool were not abnormally large in 1999 – 2001. If the dead biomass pool is indeed losing carbon, mortality must have been greater than $3.1 \pm 0.6 \text{ Mg C ha}^{-1} \text{ yr}^{-1}$ in the years preceding our measurements. This suggests the site average mortality rate (1.8 %) was not unusual and probably lower than in the recent past despite the large number of tree deaths in stems > 70 cm DBH.

The mortality inputs to CWD amounts to 10.9% of the total pool size (using Chambers allometry et al. (2001a)) and translates to a CWD pool turnover rate of ~10.5 years because the ratio of total biomass to inputs is $32.6 \text{ Mg C ha}^{-1} / 3.1 \text{ Mg C ha}^{-1} \text{ yr}^{-1}$. If, hypothetically, the CWD were in fact in steady state, the decay rate would have to be $k = 0.10 / \text{yr}$, considerably lower than either Chambers' (2001a) or Summers' (1998) decay rate estimates.

Total Aboveground Biomass Pool and Flux

The size of the total aboveground pool and size of the total aboveground flux is determined by adding together the live and dead components of each pool and flux. The total

Table 4: Flux of carbon in coarse woody debris (MgC/ha/yr) at km 67, Tapajós National Forest, Brazil. Mortality is reported using three allometries to calculate biomass from measured DBHs. Decomposition numbers are reported for three densities used to convert volume measurements to biomass and two decomposition rates that indicate the fraction of mass lost each year.

<u>FLUX IN DEAD BIOMASS</u>			
<u>Inflow: mortality</u>	Allometry 1 ^a 3.1 (± 0.6)	Allometry 2 ^b 3.8 (± 1.2)	Allometry 3 ^c 4.4 (± 1.7)
<u>Outflow: decomposition rate</u>	Density group 1 ^d	Density group 2 ^e	Density group 3 ^f
Chambers (2000)= .17/yr	5.5 (± 0.6)	7.0 (± 0.7)	7.5 (± 0.7)
Summers (1998) = .15/yr	4.9 (± 0.5)	6.2 (± 0.6)	6.6 (± 0.6)
Range of Net Change	-0.5 to -4.4		

^a from Chambers *et al.*, 2000; ^b from Brown, 1997, equation 3.2.3; ^c from Brown, 1997, equation 3.2.4; ^d from Clark *et al.*, MS; ^e from Delaney *et al.*, 1998; ^f from Summers, 1998

Table 5: Pool of Carbon (MgC/ ha) in living biomass greater than 10 cm DBH and flux of Carbon (MgC/ ha/yr) in living biomass greater than 10 cm DBH. Carbon numbers for live biomass are reported for three allometries used to scale DBHs to biomass. Carbon numbers for dead biomass are reported for three densities used to convert volume to biomass.

<u>Pool: Total Above Ground Carbon</u>			
Live Biomass (n=2791)	Allometry 1 ^a 144.1	Allometry 2 ^b 154.4	Allometry 3 ^c 161.0
Dead Biomass (n=1000)	Density group 1 ^d 32.6	Density group 2 ^e 41.4	Density group 3 ^f 43.8
-----	-----	-----	-----
Total Pool Range	176.7 to 204.8		
<u>Flux: Total Above Ground Biomass</u>			
Live Flux Range	+0.5 to -0.8		
Dead Flux Range	-0.5 to -4.4		
-----	-----		
Total Flux Range	0.0 to -5.2		

^a from Chambers *et al.*, 2000; ^b from Brown, 1997, equation 3.2.3 ; ^c from Brown, 1997, equation 3.2.4; ^d from Clark *et al.*, MS; ^e from Delaney *et al.*, 1998; ^f from Summers, 1998

aboveground biomass amounts to $176.7 \text{ Mg C ha}^{-1}$ (Table 5) (using Chambers et al. (2001a) allometry and Clark et al. (MS) densities). Of the total aboveground biomass, live wood accounts for 82% of the biomass and dead wood accounts for 18% of biomass. The range for total carbon flux for all aboveground biomass was between 0.0 to $-5.2 \text{ Mg C ha}^{-1} \text{ yr}^{-1}$. Thus, the net storage of carbon at this site appears to be quite small and probably negative, releasing carbon to the atmosphere. This result is consistent with data from the dendrometer measurements and also appears to be consistent with preliminary data from the eddy flux system.

Overall, the site is extremely dynamic, showing demographic changes in the live biomass, high mortality in large trees, high growth and recruitment in small trees and large turnover rates for both live and dead biomass pools.

DISCUSSION AND CONCLUSIONS:

The km 67 site in the Tapajós National Forest was a net carbon source to the atmosphere between 1999 and 2001. The forest experienced unusually high mortality in trees > 70 cm DBH during this two year interval and may have experienced elevated mortality prior to measurement in 1999. Temporal forest dynamics may have influenced the size and flux in carbon budgets for the two year interval and long term measurements are necessary to determine the continuing carbon balance.

Live Biomass

The live biomass estimate of $\sim 150 \text{ Mg C ha}^{-1}$ falls within the range of published biomass values for moist tropical forests in the Amazon region (Table 6). The convergence of our estimate with other values indicates that the km 67 site fits within the regional biomass patterns and can be reasonably compared to other forests within the Amazon basin.

The range of the live biomass estimates for the km 67 site were $145.5 \pm 4.9 \text{ Mg C ha}^{-1}$ to $159.7 \pm 9.2 \text{ Mg C ha}^{-1}$. The individual allometric equations used to scale up to biomass exhibited a range of $\pm 5\%$ for total biomass (Table 1) and, as a result, the change in live biomass varies from storage ($+0.7 \text{ Mg C ha}^{-1} \text{ yr}^{-1}$) to release ($-0.7 \text{ Mg C ha}^{-1} \text{ yr}^{-1}$) depending on allometry. However, this does not affect the overall conclusions for the live biomass pool because the range of estimates encompasses zero and because each estimate falls within the uncertainty of the other allometric estimates. The small range of allometric estimates of biomass demonstrates that there is not a large systematic bias due to selection of allometry when scaling up to Mg C from DBH.

Table 6: A comparison of live biomass estimates for the Amazon Region, numbers reported in Mg of dry matter ha⁻¹, for this study the dry matter weight was obtained by multiplying Mg C ha⁻¹ by two.

<u>Biomass estimate</u>	<u>Location</u>	<u>Country</u>	<u>Paper cited</u>
291	<i>This study - Santarèm</i>	<i>Brazil</i>	
282	Santarèm	Brazil	Keller et al., 2001
284	Piste de Sainte-Elie	French Guiana	Chave et al., 2001
285	Rondônia	Brazil	Foster Brown et al., 1994
298	multiple sites in Amazonia	Brazil	Brown et al., 1992
309	Nouragues	French Guiana	Chave et al., 2001
312	Manaus	Brazil	Chambers et al., 2001c
314	Paragominas	Brazil	Gerwing & Farias, 2000

Table 7: A comparison of dead biomass estimates for neotropical forests, numbers reported in Mg of dry matter ha⁻¹, for this study the dry matter weight was obtained by multiplying Mg C ha⁻¹ by two.

<u>Biomass estimate</u>	<u>Location</u>	<u>Country</u>	<u>Paper cited</u>
<i>Fallen CWD</i>			
53.0	<i>This study - Santarèm</i>	<i>Brazil</i>	
30.0	Rondônia	Brazil	Foster Brown et al., 1994
33.3	multiple sites in Venezuela	Venezuela	Delaney et al., 1998
42.3	Paragominas	Brazil	Uhl & Kauffman, 1990
46.3	La Selva	Costa Rica	Clark et al., MS
53.0	Olho D' Agua	Brazil	Cochrane & Schulze, 1999
<i>Standing CWD</i>			
12.4	<i>This study - Santarèm</i>	<i>Brazil</i>	
14.8	multiple sites in Venezuela	Venezuela	Delaney et al., 1998
23.4	La Selva	Costa Rica	Clark et al., MS
26 - 75	Olho D' Agua	Brazil	Cochrane & Schulze, 1999

Dead Biomass

CWD had a relatively large standing stock measuring $32.6 \pm 2.9 \text{ Mg C ha}^{-1}$ (Table 3). At 18% of the total aboveground biomass, CWD is a significant, but not dominant, part of the total aboveground pool. This suggests that studies that ignore the presence of CWD in the total aboveground carbon pool underestimate carbon loss during deforestation and the associated inputs of carbon dioxide to the atmosphere (Foster Brown et al., 1995).

Both the fallen and standing CWD estimates fell within the range of published values (Table 7), indicating that the pool size was comparable to other regional estimates. Although the results indicate that CWD is an important and large biomass pool, the results are not as certain as one might wish because of large uncertainties when calculating CWD. Lack of site specific density numbers caused a range of $\pm 11.2 \text{ Mg C ha}^{-1}$ or $\pm 26\%$ in CWD estimates (Table 3) because published densities were used to scale up to biomass from volume. A site specific density analysis would greatly improve the estimate of dead biomass. In addition, the decay classification scheme (sound, intermediate, decayed) may also be a source of error because observers qualitatively assigned the decay class, and the percentage of pieces in each decay class for the km 67 site varied dramatically from La Selva, Costa Rica (Clark et al. (MS)) percentages.

Total Biomass

When the live and dead biomass pools are added together, the range of total aboveground dry matter is 349.6 t ha^{-1} to 396.0 t ha^{-1} . The total aboveground biomass estimate confirms the old-growth classification of the km 67 site because the estimate falls within the upper end of the range of other published values for old-growth neotropical forests: 301 t ha^{-1}

dry matter was estimated in Santarém, Brazil (Keller et al., 2001)¹, 325 t ha⁻¹ in Rondônia, Brazil (Foster Brown et al., 1994), 295 t ha⁻¹ in Olho D'Auga, Brazil (Cochrane & Schultze, 1999) and 355 and 399 t ha⁻¹ at two different sites in Rondônia, Brazil (Guild et al., 1998).

Forest Dynamics

The evaluation of forest dynamics in live biomass illustrates that there was a demographic shift over the two year interval, with large mortality in trees > 70 cm DBH and subsequent recruitment and growth of stems into the 10 cm DBH class. The site average mortality rate, 1.8 %, fell within the published range of mortality rates for 38 other neotropical forests, 0.46% to 3.08% (Swaine et al., 1987; Phillips & Gentry, 1994). However, the mortality rates for trees > 70 cm DBH was 3.6 %, significantly higher than other published estimates. Because trees > 70 cm DBH constitute a large fraction of the total biomass (Figure 5), the abnormally high mortality in these stems explains the net carbon loss in live biomass from the largest size classes (Figure 9b; Figure 10). The death of a very large tree creates gap and open light conditions. Therefore, the elevated amounts of growth and recruitment in the small size classes (Figure 9b; Figure 10) may be a result of competitive release and/or tree colonization of new gaps.

Mortality from the live biomass pool is intimately linked with the CWD flux estimate because mortality is the inflow of carbon to the pool ($CWD_{t2} = CWD_{t1} + Mortality_{(t2-t1)} - Decomposition_{(t2-t1)}$). Therefore, one might expect that higher than average inputs to CWD from the large mortality rates in trees > 70 cm DBH might cause net storage in the CWD pool. However, this does not seem to be the case because the data shows the unexpected result that

¹ Only the total live biomass was measured by Keller et al. (2001), the dead biomass was estimated as a percentage of the total live biomass.

the CWD pool releases between $-0.5 \text{ Mg C ha}^{-1} \text{ yr}^{-1}$ and $-4.4 \text{ Mg C ha}^{-1} \text{ yr}^{-1}$. This suggests that mortality must have been even larger in the past, contributing more carbon than $-3.13 \pm 0.57 \text{ Mg C ha}^{-1} \text{ yr}^{-1}$ to create a CWD pool large enough to release more carbon through decomposition than currently gained from mortality. Furthermore, the elevated recruitment and growth of trees in the smallest size class offer further evidence of past mortality. Because trees take several years to reach a DBH of 10 cm, many gaps must have been formed several years prior to measurement. The appearance of many gaps on the Landsat image (Figure 1), dating from 1997, indicates that these processes preceded the first measurements in 1999.

The causes of such increased mortality are likely to be environmental. Most trees seemed to have died standing; the mode of death analysis for trees revealed that 100% of trees > 110 cm DBH, 75% of trees > 65 cm DBH and 61% of all trees died standing. Because such a large proportion of trees died upright, wind disturbance is unlikely as a causal factor in wide-scale tree mortality. Pests, strangler figs and drought are the most common causes for standing death in trees; however, strangler figs are not a significant factor on the site because only one tree in all 20 ha was strangled over the two year period. In addition, neither pests nor pathogens are likely causes of the observed large scale tree death. Mortality resulting from pests or pathogens tends to affect one particular species of tree or clumps of trees but mortality at km 67 was spread out over many species and a large spatial area. Furthermore, there was no physical evidence in either the CWD survey or the biomass survey of insect or fungal damage. Therefore, drought is the most likely explanation for elevated tree mortality. This explanation is corroborated by climate data from the past decade; there were six years of El Niño Southern Oscillation (ENSO) events in the 1990s (Wolter, 2001) with peaks in both 1991 and 1997 that caused wide-scale drought and water stress in the Tapajós. Thus, the ENSO events of the 1990s

are the probable cause of the current elevated mortality in large trees and the assumed elevated mortality in the past.

Net Fluxes

The range of net flux estimates, 0.0 to $-5.4 \text{ Mg C ha}^{-1} \text{ yr}^{-1}$ (Table 5), indicate small release of carbon from aboveground biomass. One of the component fluxes, live biomass flux, showed no net storage or release of carbon (Table 2) and the other component flux, dead biomass flux, showed small release of carbon (Table 4). The large size of the gross fluxes (Table 2) and pools (Table 5) fit the general observation that the tropics are a dominant proportion of terrestrial biomass (Dixon et al., 1994) and that they annually cycle a large volume of carbon dioxide (Malhi & Grace, 2000).

Two components of net flux, mortality and decomposition suffer some uncertainties and may affect confidence in the estimate. Mortality had a sampling error over 10%, reflecting large variation that could be spatial and/or temporal. In Costa Rica, 15-fold spatial variation of mortality rates was observed across a topographical and edaphic gradient (Clark et al., MS). Even in the relatively homogeneous km 67 site, spatial variation may play a role in the estimate of mortality rate and, consequently, a larger sample size might improve the estimate. However, mortality is also known to be an episodic event closely tied to climatic variation that causes drought and wind (Clark et al., MS). Therefore, mortality may be operating on a regional scale, and in this case, larger plots would not necessarily improve the estimate. Instead, repeated measurements over a longer time scale may be required to accurately characterize mortality.

Decomposition also has significant uncertainties because it was calculated from published k-constants and the CWD estimate. This means it suffers the same errors as the CWD pool and the true decay k-constant for the site is unknown. The estimate could be improved by

long term measurements of biomass loss in CWD and the establishment of a site specific decay constant.

Our net flux result of a small carbon release to the atmosphere differs from earlier eddy covariance studies (Malhi, 1998; Grace et al., 1995), ecosystem models (Chambers et al., 2001b; Tian et al., 2000) and biomass increment studies (Phillips et al., 1998). These studies estimated a neotropical carbon sink between 0.2 Gt C/yr (Tian et al., 2000; Chambers et al., 2001b) and 2.95 Gt C/yr (Malhi et al., 1998). There are a few possible explanations for why the km 67 site shows net carbon release when other papers suggest a net carbon sink. First, an unmeasured biomass pool could be storing carbon while the live and dead biomass pools are not. Second, episodic forest dynamics (such as mortality) measured over a short time interval might show net carbon release (as this paper suggests) or net carbon storage (Malhi et al., 1998; Grace et al., 1995) though the system may be at a different carbon balance over a longer time period.

Carbon storage in an unmeasured biomass pool (litter, vines, coarse roots, soil) is unlikely to be sufficient to change the sign of the net system flux. Fluxes within these other components should be small over two years because the associated pool sizes are small. For example, the litter pool could potentially serve as a carbon sink; however, the small size and rapid turnover rate makes significant storage unlikely. For other Amazonian sites, litter is only 3.4 % of total biomass (DeCamargo et al., 1999) with a pool size of 4.5 Mg C/ha and a turnover rates of < 1 yr (Trumbore et al., 1995). Carbon storage in below ground structures (coarse roots) is possible but also unlikely. The pool size is rather small because coarse roots amount to only 5% of live biomass in the tropics (Higuchi, 1997) and large storage in a small pool is improbable. Carbon storage in lianas is another possibility, but again, lianas are a small carbon pool, only 14% of total biomass in French Guiana (Gerwing & Farias, 2000). Carbon storage in

lianas is associated with changes in forest stature (Gerwing & Farias, 2000) not apparent on the Tapajós site. Soil carbon pool is a more likely candidate for carbon storage because it is a large carbon pool in the forest and modeling studies predict some carbon uptake in this pool (Tian et al., 2000). The soil carbon is approximately the same size as the living biomass pool (Malhi et al., 1999), but it has a long turnover time and a small annual flux. Although it is possible that soil organic matter is affecting the carbon budget, it is likely that the influence of the live and dead pools was far more significant than the other pools over this two-year period because live and dead biomass have larger standing stocks and gross fluxes than all the other pools combined.

It is more likely that the ecosystem is releasing small amounts of carbon because due to elevated mortality occurring prior to and concurrent with the two-year time interval of measurement. As previously discussed, mortality and subsequent recruitment, can be erratic both spatially and temporally. Both are correlated to inter-annual climate variability and therefore the flux estimate may depend on the time frame of measurement. Over the measured interval, there was high mortality rate of 3.6% for trees >70 cm DBH, whereas mortality rates for trees >70 cm have been calculated at 0.6% (Clark & Clark, 1996b) and 1.4% (Rankin-de-Marona, 1990) in other tropical forests. Because large stems account for a significant proportion of biomass (Figure 5), the loss of a few big trees could result in carbon loss for all live biomass. However, the death of an emergent results in a gap proportional to the DBH size, and consequently small pioneer and subcanopy trees experience competitive release and quickly colonize the high light conditions, contributing carbon to the system (Clark & Clark, 1996b). These two correlated events account for no net storage or release of carbon in the live pool, but also account for the size class specific changes in live flux: carbon loss from large size classes

balanced by net carbon gain in small size classes (Figure 10). The temporal variability of mortality also accounts for small release of carbon in the CWD flux. Measurements indicate a period of large mortality preceding 1999 (see forest dynamics section). There is a small flux of carbon to the atmosphere as CWD decays and recovers from this episode of elevated mortality. In the future, the carbon balance may temporarily shift to net carbon storage as the forest recovers from an episode of unusually high emergent mortality because the subsequent re-growth within the gap can serve as a carbon sink for decades (Harmon, 1991). Recruitment, mortality and standing stocks should be monitored over the next several years to test this hypothesis.

Conclusions

Over the measurement period, 1999 - 2001, the km 67 site in the Tapajós was a net carbon source to the atmosphere. However, evidence of a demographic shift suggests that the forest may not continue to be a source. Mortality and recruitment vary over longer time periods than the two-year window of measurement. Therefore, long-term measurements are imperative to determine the continuing carbon flux of this primary tropical forest.

The conclusion that this old-growth neotropical forest is a net carbon source to the atmosphere conflicts with previous studies that report a net carbon sink in primary neotropical forests (Phillips et al., 1998; Malhi et al., 1998; Grace et al., 1995; Tian et al., 2000, Chambers et al., 2001b). However, the conclusion is one data point on carbon release in a region of 5×10^8 ha that encompasses many different forest types, growing seasons and microclimates, thus it does not invalidate the results of previous papers. For this reason, no regional extrapolation of the carbon budget is attempted in this discussion. However, finding net carbon release in this neotropical old-growth forest is extremely important because it shows that carbon storage in

these forests should not be accepted as fact, and that global carbon budgets cannot be constructed with the assumption of carbon absorption in all neotropical forests.

REFERENCES:

- Ashton, P. 1998. Personal communication with Steven Wofsy.
- Brown, S. 1997. Estimating biomass and biomass change of tropical forests: A primer. United National Food and Agriculture Organization.
- Brown, S., C. A. S. Hall, W. Knabe, J. Raich, M. C. Trexler, and P. Wooster. 1993. Tropical forests: their past, present and potential future role in the terrestrial carbon budget. *Water, Air and Soil pollution* 70: 71-94.
- Brown, S. and A. E. Lugo. 1992. Aboveground biomass estimates for tropical moist forests of the Brazilian Amazon. *Interciencia* 17: 8-18.
- Chambers, J. Q., N. Higuchi, J. P. Schimel, L. V. Ferreira, and J. M. Melack. 2000. Decomposition and carbon cycling of dead trees in tropical forests of the central Amazon. *Oecologia* 122: 380-388.
- Chambers, J. Q., J. dos Santos, R. F. Ribeiro, and N. Higuchi. 2001a. Tree damage, allometric relationships, and above-ground net primary production in central Amazon forest. *Forest Ecology and Management* 152: 73-84.
- Chambers, J. Q., N. Higuchi, E. S. Tribuzy, and S. E. Trumbore. 2001b. Carbon sink for a century. *Nature* 410: 429.
- Chambers J. Q., J. P. Schimel, and A. D. Nobre. 2001c. Respiration from coarse wood litter in central amazon forests. *Biogeochemistry* 52: 115-131.
- Chave, J., B. Riera, and M. A. Dubois. 2001. Estimation of biomass in a neotropical forest of French Guiana: spatial and temporal variability. *Journal of Tropical Ecology* 17: 79-96.
- Clark, D. A., S. Brown, D. W. Kicklighter, J. Q. Chambers, J. R. Thomlinson, J. Ni, and E. A. Holland. 2001. Net primary production in tropical forests: an evaluation and synthesis of existing field data. *Ecological Applications* 11: 371-384.
- Clark, D. B. 1996a. Abolishing virginity. *Journal of Tropical Ecology* 12: 735-739.
- Clark, D. B., and D. A. Clark. 1996b. Abundance, growth and mortality of very large trees in neotropical lowland rain forest. *Forest Ecology and Management* 80: 235-244.
- Clark, D. B., D. A. Clark, S. Brown, S. F. Oberbauer, E. Veldkamp. Manuscript. Stocks and flows of coarse woody debris across a tropical rain forest nutrient and topography gradient. Accepted pending revision in *Forest Ecology and Management*.

- Cochrane, M. A., and M. D. Schulze. 1999. Fire as a recurrent event in tropical forests of the eastern Amazon: effects on forest structure, biomass, and species composition. *Biotropica* 31: 2-16.
- Cochrane, M. A. May 31, 2001. Email to Elizabeth Hammond Pyle.
- De Camargo, P.B., S. E. Trumbore, L. A. Martinelli, E. A. Davidson, D. C. Nepstad and R. L. Victoria. 1999. Soil carbon dynamics in regrowing forest of eastern Amazonia. *Global Change Biology* 5: 693-702.
- Delaney, M., S. Brown, A. E. Lugo, A. Torres-Lezama, and N. B. Quintero. 1998. The quantity and turnover of dead wood in permanent forest plots in six life zones of Venezuela. *Biotropica* 30:2-10.
- Dixon, R. K., S. A. Brown, R. A. Houghton, A. M. Solomon, M. C. Trexler, and J. Wisniewski. 1994. Carbon pools and flux of global forest ecosystems. *Science* 263: 185 – 190.
- Fan S. M., M. Gloor, J. Mahlman, S. Pacala, J. Sarmiento, T. Takahashi, and P. Tans. 1998. A large terrestrial carbon sink in North America implied by atmospheric and oceanic CO₂ data and models. *Science* 282: 442-446.
- Foster Brown, I., L. A. Martinelli, W. W. Thomas, M. Z. Moreira, C. A. C. Ferreira, and R. A. Victoria. 1995. Uncertainty in the biomass of Amazonian forests: an example from Rondonia, Brazil. *Forest Ecology and Management* 75:175-189.
- Gerwing, J. J., and D. L. Farias. 2000. Integrating liana abundance and forest stature into an estimate of total aboveground biomass for an eastern Amazonian forest. *Journal of Tropical Ecology* 16: 327-335.
- Grace, J., J. Lloyd, J. McIntyre, A. C. Miranda, P. Meir, H. S. Miranda, C. Nobre, J. Moncrieff, J. Massheder, Y. Malhi, I. Wright, and J. Gash. 1995. Carbon dioxide uptake by an undisturbed tropical rain forest in southwest Amazonia, 1992 to 1993. *Science* 270: 778-780.
- Guild, L. S., J. B. Kauffman, L. J. Ellingson, D. L. Cummings, and E. A. Castro. 1998. Dynamics associated with total aboveground biomass, C, nutrient pools, and biomass burning of primary forest and pasture in Rondonia, Brazil during SCAR-B. *Journal of Geophysical Research* 103:32,091-32,100.
- Harmon, M. E. and C. Hua. 1991. Coarse woody debris dynamics in two old-growth ecosystems. *BioScience* 41: 604-610.
- Harmon, M. E., and J. Sexton. 1996. Guidelines for measurements of woody detritus in forest ecosystems. Publication No.20. Seattle, WA: U.S. LTER Network Office, University of Washington.

- Higuchi N., J. B. S. Ferraz, L. Antony, F. Luizao, R. Luizao, Y. Biot, I. Hunter, J. Proctor, and S. Ross. 1997. Manaus, Brazil: BIONTE Biomassa e nutrientes. INPA.
- Houghton, R. A. 1991. Tropical deforestation and atmospheric carbon dioxide. *Climatic Change* 19: 99 – 118.
- Keeling, R.F., S. C. Piper, and M. Heimann. 1996. Global and hemispheric CO₂ sinks deduced from changes in atmospheric O₂ concentration. *Nature* 381: 218-221.
- Keller, M., M. Palace, and G. Hurtt. 2001. Biomass in the Tapajos National Forest, Brazil- examination of sampling and allometric uncertainties. *Forest Ecology and Management* 154: 371-382.
- Malhi, Y., D. D. Baldocchi, and P. G. Jarvis. 1999. The carbon balance of tropical, temperate and boreal forests. *Plant, Cell and Environment* 22: 715-740.
- Malhi, Y., and J. Grace. 2000. Tropical forests and atmospheric carbon dioxide. *Tree* 15: 332-336.
- Malhi, Y., A. D. Nobre, J. Grace, B. Kruijt, M. G. Pereira, A. Gulf, and S. Scott. 1998. Carbon dioxide transfer over a central Amazonian rain forest. *Journal of Geophysical Research* 103: 593-531.
- Melillo, J. M., R. A. Houghton, D. W. Kicklighter, and A. D. McGuire. 1996. Tropical deforestation and the global carbon budget. *Annual Review of Energy in the Environment* 21: 293 – 310.
- Melillo, J. M., A. D. McGuire, D. W. Kicklighter, M. I. B., C. J. Vorosmarty, and A. L. Schloss. 1993. Global climate change and terrestrial net primary productivity. *Nature* 363: 234-240.
- Parotta, John A., J. K. Francis, and R. R. de Almeida. 1995. *Trees of the Tapajos: A photographic field guide.* (General Technical Report IIRF-1) Rio Piedras, Puerto Rico: United States Department of Agriculture.
- Phillips O. L., and A. H. Gentry. 1994. Increasing turnover through time in tropical forests. *Science* 263: 954 – 957.
- Phillips O. L., Y. Mahli, N. Higuchi, W. F. Laurance, P. V. Nunez, R. M. Vasquez, S. G. Laurence, L. V. Ferreira, M. Stern, S. Brown, and J. Grace. 1998. Changes in the carbon balance of tropical forests: evidence from long-term plots. *Science* 282: 439-442.
- Prentice, I. C., G. D. Farquhar, M. J. R. Fasham, M. L. Goulden, M. Heimann, V. J. Jaramillo, H. S. Khesghi, C. Le Quere, R. J. Scholes, D. W. R. Wallace. 2001. The Carbon Cycle and Atmospheric Carbon Dioxide. In J. T Houghton et al., editors. *Climate Change 2001: the Scientific Basis.* 183 – 237. Cambridge: Cambridge University Press.

- Rankin-de-Merona, J. M., R. W. Hutchings, and T. E. Lovejoy. 1990. Tree mortality and recruitment over a five-year period in undisturbed upland rainforest of the Central Amazon. In A. Gentry editor. *Four Neotropical Rainforests*. 19 – 33. Chicago: University of Chicago Press.
- Salati, E., and P. B. Vose. 1984. Amazon basin: a system in equilibrium. *Science* 225: 129-138.
- Summers, P. M. 1998. Estoque, decomposicao, e nutrientes da liteira grossa em floresta de terra-firme, na Amazonia central. MS thesis. Instituto Nacional de Pesquisas da Amazonia, Manaus, Brazil.
- Swaine, M. D., D. Lieberman, and F. E. Putz. 1987. The dynamics of tree populations in tropical forest: a review. *Journal of Tropical Ecology* 3:359 – 366.
- Tian, H., J. M. Melillo, D. W. Kicklighter, A. D. McGuire, J. Helfrich III, B. Moore III, and C. J. Vorosmarty. 2000. Climatic and biotic controls on annual carbon storage in Amazonian ecosystems. *Global Ecology and Biogeography* 9:315-335.
- Trumbore, S. E., E. A. Davidson, P.B. de Camargo, D. C. Nepstad, and L.A. Martinelli. 1995. Belowground cycling of carbon in forests and pastures of Eastern Amazonia. *Global Biogeochemical Cycles* 9: 515-528.
- Uhl, C., and R. Buschbacher. 1985. A disturbing synergism between cattle ranch burning practices and selective tree harvesting in the eastern Amazon. *Biotropica* 17: 265-268.
- Uhl, C., R. Buschbacher, and E. A. S. Serrao. 1988. Abandoned pastures in eastern Amazonia. I. patterns of plant succession. *Journal of Ecology* 76: 663-681.
- Uhl, C., and J. B. Kauffman. 1990. Deforestation, fire susceptibility, and potential tree responses to fire in the eastern Amazon. *Ecology* 71: 437-449.
- Wolter, K. 2001. Multivariate ENSO index (MEI). [Online: web]. Updated December 5, 2001. Cited December 19, 2001. URL: <http://www.cdc.noaa.gov/enso/>